C.P. No. 1145

C.P. No. 1145

MINISTRY OF AVIATION SUPPLY

AERONAUTICAL RESEARCH COUNCIL

CURRENT PAPERS

Two-Dimensional Low-Speed Tunnel Tests on the NACA 0012 Section Including Measurements Made During Pitching Oscillations at the Stall

by

G. F. Moss and P. M. Murdin

Aerodynamics Dept, R.A.E., Farnborough

LONDON: HER MAJESTY'S STATIONERY OFFICE

1971

PRICE *60p* NET

U.D.C. 533.692 : 533.6.013.13 : 533.6.071 : 533.6.011.32/34 :
533.6.013.152 : 629.13.038.1

CP No. 1145*
May 1968

TWODIMENSIONAL LOW-SPEED TUNNEL TESTS ON THE N.A.C.A. 0012 SECTION INCLUDING MEASUREMENTS MADE DURING PITCHING OSCILLATIONS AT THE STALL

by

G. F. Moss
P. M. Murdin

SUMMARY

Lift measurements were made on a 10% thick N.A.C.A. 0012 section under static conditions and during pitching oscillations in an attempt to provide sectional data for use in calculations on helicopter rotors. Strong threedimensional effects were found at the stall, however, which seemed to be inherent in the aerodynamics of the stall itself. Also, the cyclic variation of lift during the pitching oscillations was found to be intermittent between two distinct types during both of which considerable hysteresis was observed and during one of which very large increases in maximum lift were encountered.

*Replaces RAE Technical Report 68104 - ARC 30 682

CONTENTS

1 INTRODUCTION

The work described in this Report was carried out at a time when experimental and analytical investigations being made by Naval Air Department, R.A.E.[1,2], were showing clearly for the first time the large discrepancies between the lift developed in practice by a helicopter rotor and that which could be explained by the use of twodimensional strip theory with the inclusion of well established static aerofoil characteristics[3,4]. In the first instance the blades were taken to be infinitely stiff and a constant induced velocity over the span was assumed. The non-linear aerofoil characteristics, however, were included and the spanwise flow effects on drag were allowed for. However, large discrepancies between these calculations and experimental measurements of thrust were apparent at conditions when partially stalled areas within the rotor disc were to be expected from the steady aerofoil data. The only explanation possible was that for the threedimensional unsteady conditions of a lifting rotor very much higher sectional $C_{L_{max}}$ values were possible than for twodimensional steady conditions at the same Reynolds number, Mach number and surface conditions. Experiments showed that the flapping and torsional oscillations were small enough to be discounted as insignificant in themselves and the large centrifugal forces acting on surface boundary layers were not expected to account for more than a small part of this discrepancy[5]. Together with this experimental and analytical work at R.A.E., similar problems were being investigated concurrently in the U.S.A.[6].

For the case of forward flight at high thrust conditions, the above strip theory predicts an asymmetric distribution over the rotor disc with a region of low dynamic head, high incidence and high lift-coefficient directly to one side of the disc (at 270° azimuth). However, such experimental evidence that was available[7,8] clearly indicated on analysis[1] that this region of high lift-coefficient occurs well forward of the transverse axis on the retreating-blade side (at 230°-240° azimuth) and that in addition a region of comparatively low lift-coefficient occurs at an aft point on the same side (at about 300° azimuth). In these investigations the local maximum lift-coefficients reached were about 60% in excess of the usual steady two-dimensional values at corresponding conditions and the integrated thrust for the whole rotor was much higher also.

To obtain agreement between these calculations and experimental results, therefore, it was necessary to assume that a considerable extension of the local lift-incidence curve was occurring accompanied by a large amount of cyclic hysteresis. In addition to the unsteady aerodynamic conditions due to the rotation of the blades in forward flight, sectional oscillations in heave, pitch and in a chordwise direction were known to be taking place. Although it was well known at the time that such oscillations could results in an increase in $C_{L_{max}}$ accompanied by considerable hysteresis, the available data was limited in usefulness for the range of conditions under consideration. The work by Halfman et al[9] on oscillating aerofoils of arbitrary shape, however, does show that a large increase in normal-force coefficient is possible and that extensive hysteresis loops in sectional pitching-moment can occur. The investigations on a N.A.C.A. 0012 aerofoil oscillating in pitch by Carta[10] have a more direct bearing on the rotor problems since this is the section most often used for helicopter blades, but this data did not become available until well after the start of the experimental work described here and on subsequent analysis[1] could only explain the cyclic distortions in azimuth of the load distribution and not the large discrepancy in the level of lift-coefficients.

This was because although the hysteresis loops in lift-coefficient were large and the transient value of $C_{L_{max}}$ was well above the steady state value, the loops were equally disposed about the lift-incidence curve for steady conditions so that little or no overall increase in lift was indicated.

So little unsteady twodimensional data was available for the calculations that any experimental work by R.A.E. was thought to be of use either directly in the theory or indirectly as a means of furthering our understanding of the aerodynamics involved. It was realized from the start that it was quite out of the question to obtain comprehensive data for the extremely wide range of incidence and Reynolds number which applies to the helicopter blade section, or to try to cover all the various unsteady motions which occur in flight. The attempt was made, therefore, to obtain lift and pitching-moments during pitching cycles at high mean incidence for a twodimensional wing of N.A.C.A. 0012 section. Two series of experiments were made in the R.A.E. Bedford 15ft × 9ft low speed wind tunnel during February 1963 and January 1964 respectively. The first of these is

only briefly referred to here by way of completeness, and in fact the limited findings were repeated and largely confirmed by the later work which is described in full.

2 DETAILS OF TESTS

(a) Apparatus

The general arrangement of the wing in the tunnel is shown in Fig.1. The wing, which was of laminated spruce construction with a reinforced resin skin, was 12% thick with a chord of 16 inches and a span of 60 inches. In the preliminary series of tests the wing was fitted with end plates, 32 inches long by 16 inches deep, but in the main series circular end plates of 32 inches diameter were used centred on the pitching axis of the wing at 25% chord. These large circular plates fitted flush into two false walls in the tunnel working section which were 1 inch thick and 124 inches long. A one-inch overlap labyrinth seal was used between the circular end plates and the false walls, and the gaps were controlled to 0.05 inch by bracing wires to the tunnel walls at the pitching axis of the wing. The leading-edge of the wing was approximately 40 inches or $2\frac{1}{2}$ wing-chords from the leading-edge of the false walls. The photographs in Figs.2 and 3 show the wing in the tunnel with both end-plate arrangements. For the main series of tests with false walls, it was found necessary to fit light struts between cleats at the end plates and the foot of the main support strut in order to avoid judder and buffet when the wing was oscillating into and out of heavily stalled conditions. The main support strut was vertical and was mounted on a stiff strain-gauge balance system below the working section. At the top of this strut the wing was attached at the 25% chord point inside the thickness of the section by means of a pair of crossed-spring pivots on a spreader bar. The wing was free to oscillate without friction or mechanical interference from the rig and interference-free vertical forces in the support strut were obtained. The pitching oscillations were achieved by means of a light rear strut and an adjustable sting connected to the underside of the wing. A crossed-spring pivot was also used for the rear-strut/sting connection and this was always kept at the same height as the wing pivots for the mean incidence of each pitching oscillation tested in order to avoid undue harmonic distortion in the motion. Both the main support

strut and the rear forcing strut were shielded from the wind. Initially it had been intended to measure the vertical forces also in the rear strut, but this was abandoned because of the mechanical 'noise' content in the strain-gauge signal. Thus only the aerodynamic forces on the wing sensed by the vertical freedom of the forward strut have been considered reliable enough to present here. Since the pivot in the wing was at 25% chord, however, only small differences from total lift are likely, and for convenience the forces have been presented as lift coefficients. The possible errors inherent in this assumption are discussed in section 2(c).

Details of the balance and oscillating rig are given in Fig.4 and a photograph is shown in Fig.5. The forward strut was restrained laterally by spring-pivoted linkages at 'A' and 'B' which were accurately aligned so that the large variations in wing drag and rolling-moment (which sometimes occurred when the wing was partially stalled) had no interaction on the vertical force measured. The vertical force was measured by the spring-pivoted lever bar and strain-gauged strip shown in Fig.4. This strip could be moved along the bar to keep sensitivity to a maximum and the unwanted dead-weight loads of the strut and model were cancelled by a balance weight also attached to this lever bar. After trying many schemes, the best method of cancelling the inertia forces was found to be the spring-pulley-wire system shown in Fig.4. The spring stiffness was changed for each rate of oscillation and no attempt was made to do more than reduce the 'wind-off' signal to a reasonably small value.

The rear strut was forced by means of a mechanism comprising parallel slides, an eccentric crank with an adjustable throw, a heavy flywheel and a variable speed electric drive. This mechanism produced pure harmonic motion with amplitudes up to $\pm 1\frac{1}{2}$ inches (i.e. $\pm 2.83^{\circ}$ oscillating incidence on the wing) at frequencies up to 5 cps.

Static measurements of lift and pitching-moment were also made using the strain-gauge system for the forward strut described above and an auxiliary similar system in the rear strut.

(b) Data recording

For the static tests the strain-gauged balances on the forward and rear struts were connected in the usual way to standard ac bridge-servo units.

For the main oscillatory tests, however, a dc system was used and the signals from the forward strut balance were, after amplification, fed into a Honeywell BB 130 galvanometer used in conjunction with an N.E.P. 1050 ultra-violet light recorder. The frequency response of the galvanometer was found to be independent of signal amplitude and within the range of this experiment the phase lag was negligible, the error being about 0.1 degrees at the highest oscillation frequency tested at 4.9 cps. The full width of the trace was used during each test by adjusting the signal sensitivity and by using a shunt resistor in the strain-gauge bridge to cancel the mean aerodynamic load. Both these controls were carefully calibrated for each test. The instantaneous position of the wing throughout the pitching angle was indicated on the recorder trace by means of signals from a photo-electric cell adjacent to a light source, interrupted by a slotted disc attached to the flywheel of the forcing machanism. An indication on the trace for every 15° of crank movement was given, and in general the traces were analysed by reading ordinates at these intervals to avoid any errors due to small variations in the trace feed rate.

In the preliminary series of tests with this wing, considerable difficulties were encounted with the instrumentation. Far more mechanical noise and aerodynamic buffet was apparent in the signal than had been anticipated, and the data recording system using a somewhat more sophisticated ac system had to be damped a little to produce readable trace records. The necessary harmonic corrections to these results proved to be too unreliable as well as being difficult to apply, and the decision was taken to repeat the tests with simpler and more direct instrumentation and to take the opportunity of improving the rig in other respects, including the incorporation of false walls instead of end-plates for the wing. However, some typical results of this first series of tests are given in Fig.6 for interest.

(c) Experimental method

Because of the unpredictable nature of the lift loads and the need to obtain as high an accuracy as possible, the experiment was carried out as a series of short runs each complete in itself. For each test condition a spring of appropriate stiffness was fitted to the inertia cancelling system to keep the amplitude of the 'wind-off' recorder trace to a minimum. Then

with the wind speed set to the selected value, the zero-shift and sensitivity potentiometers were adjusted to give the maximum trace amplitude on the recorder for a series of cycles over a period of time. Finally with the wind stopped 'zero' traces were recorded and calibrations were made with dead weight loads and springs attached to the model sting in order to interpret these potentiometer settings in terms of lift load. Both the wind-off and wind-on traces were then measured to a datum at every 15° of crank position and the differences used to obtain a plot of lift load throughout the series of wind-on cycles. Part of a typical record with the wind-off and wind-on traces superimposed is given in Fig.10.

The wind speed in the tunnel was assumed to be constant throughout the oscillatory cycles and no attempt was made to control or measure the small cyclic variations that must have occurred as the drag of the model varied. However, at the higher oscillatory speeds the considerable inertia of the airsteam in the circuit of this tunnel (700 000 cu ft approximately) helped to maintain constant conditions for the working section as a whole, and at the lower oscillatory speeds the particularly rapid fan-speed control on this facility was useful in this respect. Of more significance was the possibility of cyclic variation of the velocity distribution across the working section. Checks made, however, at quasi-static conditions with pitot statics in the channels outside the false walls showed that the cyclic variation in dynamic head at the model must have been within $\pm 1\%$ of the average value used for the calculation of coefficients. After detailed calibration of the flow across the working section, a pitot-static tube positioned above and ahead of the model was used for monitoring purposes. A continuous check was also kept during the tests with an array of yawmeters along the leading-edges of the false walls. The tunnel speed itself was controlled with the normal static tapping in the working section which, with the very long working section of this facility, was well ahead of the rig.

No corrections for wall-constraint on incidence or blockage on wind speed have been applied to the experimental results, since these corrections were found to be small enough to ignore both as regards the mean conditions and the variations within the oscillatory cycles. The overall accuracy of the results was largely determined by the basic difficulty in measuring the

traces accurately and the unsteady nature of the lift load under stalled and partially stalled conditions. This overall accuracy may be taken as about ±3 or 4% and is thus very much larger than any possible blockage or incidence-constraint corrections.

Static measurements were also taken with the forcing crank stopped every 15° throughout a complete cycle, and in these tests the force in both forward and rear supporting struts was recorded enabling pitching moments to be computed. During these static tests, a check was made of the effect of varying the gap at the labyrinth seal round the edge of the circular end-plates. No effect on measured forces was observed.

As has been mentioned in section 2, the measurement of forces in the rear forcing-strut had to be abandoned for the oscillatory tests, and thus only the coefficient of the vertical force at the 25% chord point on the wing has been presented here ($C_{L_{0.25c}}$). However, reference to Figs.7 and 8 which give the variation of static pitching moment coefficient about this axis, shows that the larger numerical values are only associated with heavily stalled conditions when the lift-coefficient is comparatively small. Thus the lift coefficients measured at 25% chord, $C_{L_{0.25c}}$, may be regarded as within −0.015 of total C_L just before the stall and within +0.04 of total C_L at completely stalled conditions. This means that the plots of $C_{L_{0.25c}}$ show a slightly smaller loss of lift due to the stalling process than would be given by plots of overall lift coefficient.

(d) Model configurations

The wing was tested in three conditions, with transition free, transition fixed and with a spanwise array of vortex generators along the upper surface. With transition free, the transition position at the high incidences of these tests occurred at the reattachment point aft of the laminar separation bubble near the leading-edge on the wing upper-surface. This bubble was, of course, very much more in evidence at the lower wind speed. At these high incidences the leading-edge stagnation point was well back on the lower-surface leading-edge and it was found difficult to trip transition in the strong favourable pressure gradients ahead of this. Transition was thus fixed by a roughness band of sparsely distributed 0.004 inch particles placed between the leading-edge and the 10% chord

line on the upper surface. This band was just effective at the lower wind speed of the tests. The vortex generators used were placed in a counter rotating array along the 10% chord line on the upper surface of the wing. Each generator comprised a small square piece of thin sheet metal of size 0.25 inch × 0.25 inch inclined at 20° to the stream direction distributed at a pitch of 0.75 inch in the spanwise direction.

(e) Test programme

For all the three conditions of the wing mentioned in the last paragraph, the tests were made at two wind speeds, 100 and 200 ft/sec, giving chord Reynolds numbers of 0.84 and 1.68×10^6 respectively. Five rates of oscillation were used, 0.125, 1.06, 1.77, 3.14 and 4.42 cycles/sec in addition to static tests. These five oscillation rates corresponded to reduced frequencies (defined as $\frac{2\pi f c}{V}$) of 0.0096, 0.080, 0.150, 0.234 and 0.369 at the wind speed of 100 ft/sec, and 0.048, 0.040, 0.075, 0.117 and 0.185 at the wind speed of 200 ft/sec*. The full amplitude of oscillation, $\pm 1\frac{1}{2}$ inches, available with the forcing mechanism was used for the main bulk of the tests and gave an amplitude in incidence for the wing of ±2.83°. However, at a wind speed of 100 ft/sec with transition free some additional tests were made with an amplitude of ±0.96°, i.e. approximately one third of the above value. The mean incidence of each test run was chosen to be as high as possible but not so high that at the lowest incidence in the oscillatory cycle the wing had too small a chance of recovering to an unstalled condition. This choice of incidence range was made by trial and error, and once made was not varied as a test parameter. These incidence ranges were 10.95° to 16.60° for the wing with transition free and fixed, and 13.42° to 19.07° for the wing with vortex generators*. The additional test with reduced amplitude had an incidence range of 12.8° to 14.72°.

---

*For the first test series briefly referred to in section 3 and in Fig.6 only, a reduced frequency of 0.075 rather than 0.080 was used at a wind speed of 100 ft/sec. The incidence range was also not quite the same, 12.8° to 18.6°.

3 RESULTS AND DISCUSSION

(a) Preliminary test series measurements

A typical example of the results obtained in the preliminary test series is given in Fig.6. The full-line curve shows the static variation of lift with the large hysteresis loop which occurred at this lower wind speed with free transition. When incidence was varied between 12.8° and 18.6° at a reduced frequency of 0.75, two distinct types of lift variation were found. In the first of these the static stall was delayed resulting in an increase in $C_{L_{max}}$, the remainder of the cycle being substantially the same as the static case. In the second type of variation attached flow failed to re-establish itself as incidence was decreased, resulting in a cycle with the wing virtually completely stalled throughout. During a large number of successive cycles these two types of variation occurred intermittently without any obvious pattern apart from a tendency for each type of cycle to appear in batches rather than singly. At higher oscillatory speeds the 'high lift' cycle included progressively less and less stalled flow, becoming at the highest frequency at flat almost closed loop extending the static lift curve. The 'stalled' type of cycle, however, tended to include more mixed flow conditions at the higher frequencies, resulting in more hysteresis. These frequency effects are discussed below in the context of the main test series.

During these tests, also, it was found impossible to obtain a proper twodimensional stall on the wing. The sectional stall was basically of the trailing-edge type, as might be expected for this profile at these Reynolds numbers, and the first breakdown of flow usually occurred towards the middle of the wing span where there was presumably a small local upwash interference from the main support strut. Strong threedimensional flows developed after this initial separation which at first was thought to be entirely associated with the use of end plates and other threedimensional elements in the model rig. These two unexpected findings, the non-periodic nature of the flow and the threedimensional stall development, prohibited the use of the data directly in the strip-theory calculations mentioned in section 1. However, both these effects were confirmed in the later series of tests and must be regarded as genuine aerodynamic features of a twodimensional condition.

(b) Static measurements

The static variation of lift for the variations of incidence used in the oscillating tests is given in Fig.7 for the three conditions of the wing and the corresponding pitching moments are given in Fig.8. For the wing with free transition, a laminar-separation bubble followed by reattachment formed at the leading edge of the wing at incidences well below the stall, and this was more extensive at the lower of the two wind speeds. This bubble was absent with the roughness band present, but as was expected with a 'trailing-edge' type of stall, $C_{L_{max}}$ occurred earlier in the incidence range due to the artificial thickening of the upper-surface boundary layers. The reduction of $C_{L_{max}}$ at 200 ft/sec due to the roughness band was severe, but at the lower speed, when the size of roughness was only marginally big enough to cause transition at the leading edge, this adverse effect was only small. The most significant effect of adding the roughness band therefore was the suppression of the large hysteresis loop in the variation of lift which was present at the lower wind speed with free transition. As might be expected with a 'trailing-edge' stall, the addition of the vortex generators, although probably not of the optimum design possible, had a marked effect on the stalling angle and the size of $C_{L_{max}}$. The stall, however, was preceeded by a gradual loss of lift and was itself very violent in nature, a very large loss of lift being caused. For this configuration there was virtually no hysteresis in lift although the laminar-separation bubble persisted at incidences right up to the stall.

Oil photographs of the wing upper surface flow are shown in Fig.9 at selected incidences. There was considerable adverse scale effect at wind speeds below those used in the tests, and as a result the oil patterns were subject to abrupt changes of flow as the wind was reduced to zero prior to taking the photographs. Thus some of the patterns are blurred and this is particularly noticeable for the partially stalled conditions. The flow photograph with vortex generators present at the pre-stall incidence of 14.2° is also slightly affected. However, these flow photographs do show the marked threedimensional stall development which was also found in the preliminary test series (see section 3a). Referring to the curve for transition - free conditions in Fig.7b and the corresponding flow

studies in Fig.9a, a gradual rounding of the lift-incidence curve occurred at high incidence culminating in a sudden loss of lift at the stall at an incidence near 14°. This loss was due to a very rapid forward movement of a rear separation at one local spanwise position rather than a general separation over the whole span as might have been expected. The small local interference at the position of the support strut was presumably sufficient to trip the separation first mid-span and the part-span vortices at the edges of this initial stalled region caused an increase in downwash at the trailing-edge on either side, thus reducing the rate of spread and finally stabilizing a partially stalled condition ($\alpha = 14\frac{1}{2}^{\circ}$). As incidence was further increased, the spanwise spread of the separation along the trailing edges was inhibited by these strong port-span vortices and only a small further loss of lift occurred. However, at about $16\frac{1}{2}^{\circ}$ of incidence the separation reached one of the false walls which was then 'incorporated' as a boundary of the stall-wake, and a further large loss of lift was evident. This initial rapid loss of lift followed by a gradual loss as incidence is increased and then perhaps by a further rapid loss, gives a shape of lift-incidence curve which is often a characteristic of so-called twodimensional aerofoil data, (e.g. Ref.4). With transition fixed (Fig.9b) the initial rapid loss of lift at the stall was more severe and the separated region spread spanwise almost at once to one of the false walls. By about 15° of incidence the stall had spread across the whole wing. With vortex generators present the stall was delayed to 17° of incidence, but was preceeded by considerably more rounding of the lift-incidence curve due to the gradual deterioration of the boundary-layer at the trailing edge. The oil-flow photograph at 16.2° shows a separation near the trailing edge fairly evenly distributed across the span, but already showing a tendency to develop threedimensional characteristics. Even at 19.1° of incidence, after the very large sudden loss of lift at the stall and the subsequent rapid spanwise spread of the stall to the false walls, one small section of the wing still had attached flow due to the strong influence of the part span vortex at the edge of the wake (Fig.9c).

The implications of this threedimensional stalling behaviour under these nominally twodimensional conditions are obvious for the type of analysis techniques used on helicopter rotors mentioned in section 1. Once partially stalled conditions occur along the blade, strong threedimensional

flows are set up which make the validity of any strip-theory approach very doubtful. Also at incidences beyond the stall sectional data from other twodimensional tunnel tests of the type described here should be used with caution because of the probability of threedimensional stall development. However there is no reason to suppose that the partially stalled areas which are known to exist for the helicopter rotor in forward flight are any different in character to those found during these tunnel tests. Subsequent to the work described in this Report, similar threedimensional stalling conditions under nominally twodimensional test arrangements have also been found by Gregory et al[11].

(c) Oscillatory measurements

Two typical trace records are shown in Figs.10a and 10b and are analysed in Figs.11a and 11b respectively. Only a small number of consecutive cycles are shown in each example and for convenience the 'zero' trace (with wind-off) has been superimposed to demonstrate how the values of $C_{L_{0.25c}}$, were obtained. In the first test, Fig.10a, two 'high-lift' cycles and three 'stalled' cycles are given for transition-fixed conditions at V = 200 ft/sec and $\frac{2\pi f c}{V}$ = 0.117, and one of each of these two types has been plotted in Fig.11a with corresponding points marked, D.E.F.G. and P.Q.R.S. respectively. The scale of the trace ordinate difference Δy, is given on the side of the Fig.10a and the value of the zero-offset, ΔC_L, is also quoted. The 'stalled' cycle, P.Q.R.S., is shown in Fig.11a to be a lift-incidence hysteresis loop roughly centred on the stalled portion of the static curve, and the 'high-lift' cycle, D.E.F.G., includes portions following the lower half of the 'stalled' cycle and portions during which the wing flow almost completely reattached and high-lift coefficients were developed very much above the maximum static value attained. Usually associated with this reattached flow was a tendency for the lift curve to be extended with a comparatively high local lift slope, for which there is no immediately obvious explanation. In Fig.11a an idealized extension of the static lift-curve has been plotted which appeared to be an upper bound for the 'high-lift' cycles. The trace corresponding to this idealized curve for unstalled conditions has been reconstructed in Fig.10a.

From the example shown in Figs.10b and 11b, a test with a smaller amplitude of incidence has been chosen since this gives a clear example of a complete cycle with fully attached flow throughout. Although with transition free conditions at 100 ft/sec there would normally have been a large

hysteresis loop in the static lift-incidence curve (Fig.7a), with the reduced incidence amplitude of this example, 12.8° to 14.72°, no such hysteresis was found. Three successive cycles, A.B.C.D.E.F.G., have been analysed for the plot in Fig.11b, the portion B.C.D. being completely unstalled. This pattern of the trace record is seen to correspond to a flat loop lying along an extension of the static lift curve with a small increase of slope. The 'stalled' cycle, E.F.G., is also a flat hysteresis loop but with a large variation in lift due to marked changes in the proportion of separated flow.

The main results are summarized in Figs.12a, b and c. In each case the curve for static conditions is shown chain-dotted for comparison purposes, and the two types of lift variation, demonstrated above in the examples of Fig.11, are shown by full and dotted lines. Where only one type of cyclic variation was encountered, only one hysteresis loop is shown using a full or dotted line appropriate to whether the cycle was of the 'high lift' type or 'stalled' type respectively. Only one typical cycle in each case has been quoted, since for each type of flow variation the cyclic variations were generally very similar in character. It will be seen from Fig.12 that in all cases, whether lift-incidence hysteresis was present under static conditions or not, there was a steady increase of hysteresis as the frequency of oscillation increased. For the 'high lift' cycles there was a tendency for this hysteresis to decrease at the higher frequencies and for the rate of increase of maximum lift coefficient with frequency parameter to be reduced somewhat (see Fig.13 for a cross-plot of this). For the 'stalled' type of cycle, hysteresis again generally increased with frequency, the minimum lift in the cycle becoming smaller and the maximum lift bigger particularly at the higher frequencies. It is interesting to note that during these 'stalled' types of cyclic variation, when a significant portion of the wing upper-surface flow was always separated, it was possible at high frequencies to obtain maximum lift coefficients well in excess of the maximum value attained at corresponding static conditions. This demonstrates that the beneficial unsteady effects on lift found when the flow is everywhere attached can also occur when there are adjacent stalled areas. This could be of some significance in the context of helicopter rotor aerodynamics.

Several further comments can be made on these results taken as a whole. Firstly, the tendency for a local increase in lift slope to occur when

complete reattachment of the flow is established during the 'high-lift' cycles, is not restricted to the two examples chosen for Fig.11. Under unsteady conditions therefore the gradual loss of lift prior to the static stall, which manifests itself as a rounding of the curve, may also be recovered under dynamic conditions. Secondly, the transition from the 'stalled' type of cyclic variation back to the 'high lift' type where large areas of attached flow are re-established, usually occurred during a portion of the cycle when incidence was increasing rather than decreasing (e.g. AB of Fig.10b). Lastly, the relative numbers of 'high-lift' cycles to 'stalled' cycles which occurred in over a period of time calls for some comment. Records were usually made of at least 30 successive cycles, and this only after conditions had thoroughly settled down. As may be seen from Fig.12, in some test conditions only one type of cyclic variation was encountered; however when the two types did occur there was a general tendency for proportionally more 'high-lift' cycles to occur at the higher frequencies.

4 CONCLUSIONS

The experimental work described in this Report demonstrates that considerable increases in sectional $C_{L_{max}}$ can be achieved at low wind speeds when this aerofoil is oscillated in pitch with an amplitude of incidence which includes the static stall angle. A large amount of lift-incidence hysteresis also occurs under the dynamic conditions. However for most of the tests two distinct types of cyclic variation of lift were encountered, one with substantially unstalled conditions for much of the cycle and thus developing high lift coefficients, and the other with virtually stalled conditions throughout giving a much poorer performance. During any long succession of cycles these two types of cyclic variation appeared to be distributed with time in a fairly random manner, thus perhaps contributing a possible cause for some of the vibration problems of helicopter rotors in forward flight at high-lift conditions. The development of the stall during these tests, found to be inherently threedimensional in character, leads to the conclusion that considerable care must be exercised in the use of so-called twodimensional data in current strip theory prediction methods for helicopter rotors.

The mechanism by which such high lift coefficients can be developed in unsteady conditions is obscure and needs considerably more work before

being properly understood. Perhaps some 'pumping' action on the overall circulation is induced by the oscillatory shedding of vorticities into the stream, or perhaps there are fundamental differences between the rates of separation and re-establishment for wing boundary layers with this type of trailing-edge stall mechanism. There is no reason to doubt, however, that these tests although not giving the expected direct help with current rotor performance calculations, have none the less given some insight into the complex aerodynamic problems involved.

REFERENCES

No.	Author	Title, etc.
1	A.R.S. Bramwell E. Wilde J.B.B. Johnston	Comparison of theoretical and experimental determination of helicopter rotor characteristics with particular reference to high blade incidence conditions. R.A.E. Technical Report 66139 (1966)
2	J.B.B. Johnston	Air experimental study of helicopter rotor characteristics at tip speed ratios up to 0.5. R.A.E. Technical Report 66169 (1966)
3	R. Jones D.H. Williams	The effect of surface roughness on the characteristics of the aerofoils N.A.S.A. 0012 and R.A.F. 34. R. and M. 1708 (1936)
4	E.N. Jacobs A. Sherman	Aerofoil section characteristics as affected by variations of Reynolds number. N.A.C.A. Report 586 (1937)
5	P.J. Carpenter	Lift and profile drag characteristics of N.A.S.A. 0012 airfoil as derived from measured helicopter rotor hovering performance. N.A.C.A. Technical Note 4357 (1958)
6	G.E. Sweet J.L. Jenkins	Results of wind tunnel measurements on a helicopter rotor operating at extreme thrust coefficients and high tip speed ratios. I.A.S. Conference Paper (1963)
7	G. Falabella J.R. Meyer	Determination of inflow distributions from experimental aerodynamic loading and blade-motion data on a model helicopter rotor in hovering and forward flight. N.A.C.A. Technical Note 3492 (1955)

REFERENCES (Cont'd)

No.	Author	Title, etc.
8	J.R. Meyer G. Falabella	An investigation of the experimental aerodynamic loading on a model helicopter rotor blade. N.A.S.A. Technical Note 2953
9	R.L. Halfman H.C. Johnson S.M. Haley	Evaluation of high-angle-of-attack aerodynamic-derivative data and stall-flutter prediction techniques. N.A.S.A. Technical Note 2533 (1951)
10	F.O. Carter	Experimental investigation of the unsteady aerodynamic characteristics of a N.A.S.A. 0012 aerofoil U.A.L. Report M-1283-1 (1960)
11	N. Gregory V.G. Quincey C.L. O'Reilly D.J. Hall	Progress report on observations of three-dimensional flow patterns obtained during stall development on aerofoils, and on the problem of measuring twodimensional characteristics. N.P.L. Aero Report 1309 (ARC 31702) (1970) To be ARC CP 1146

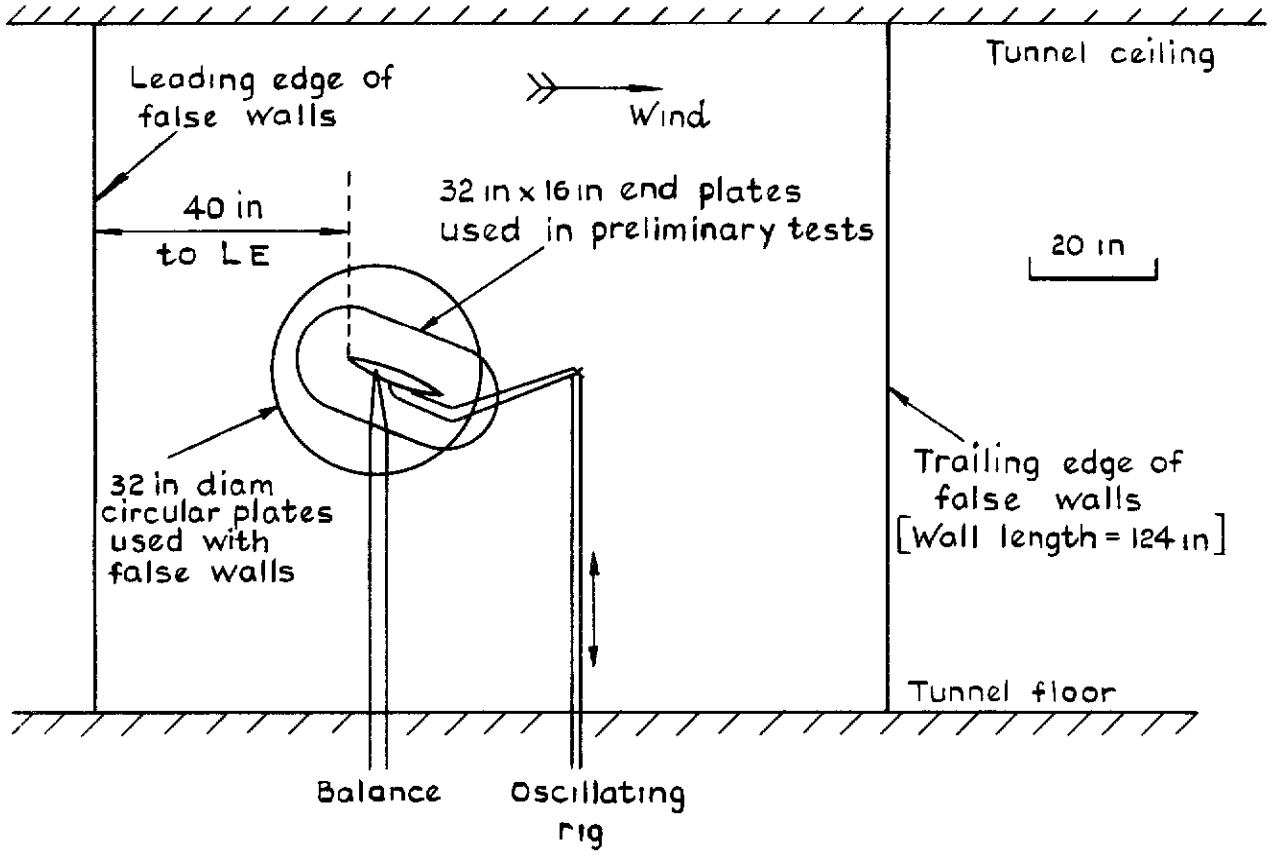

a Side view of model in working section

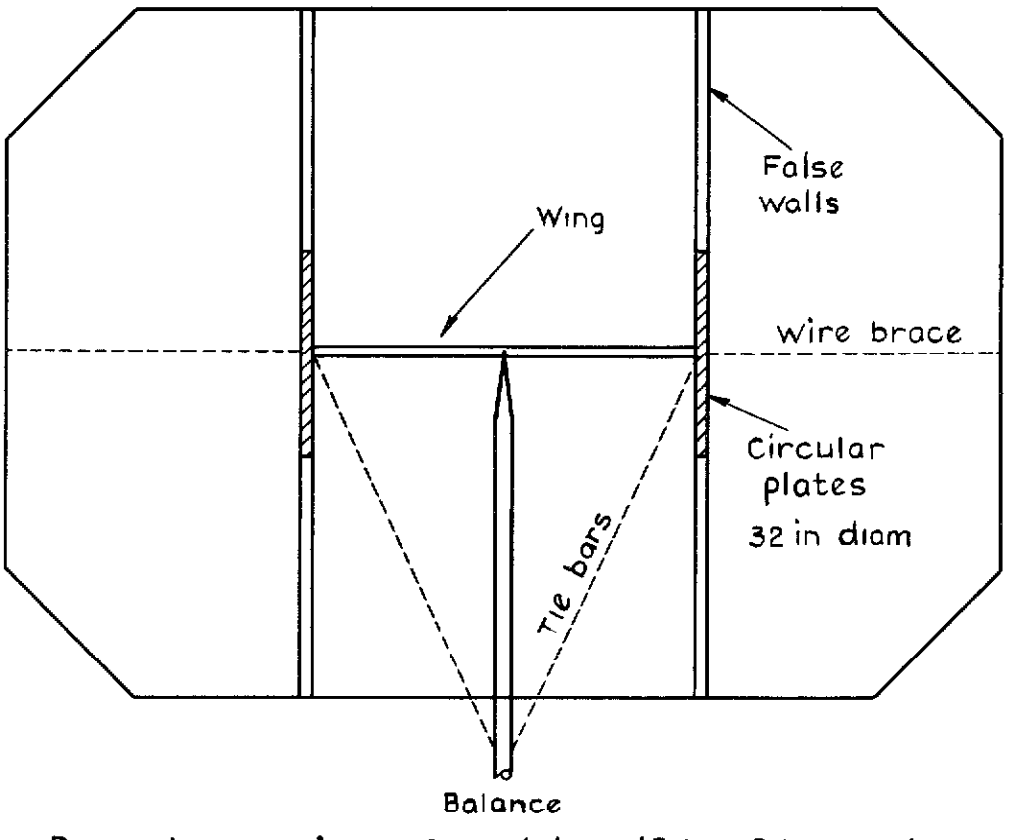

b Downstream view of model in 13ft x 9ft section

Fig 1 a & b General arrangement of model in tunnel

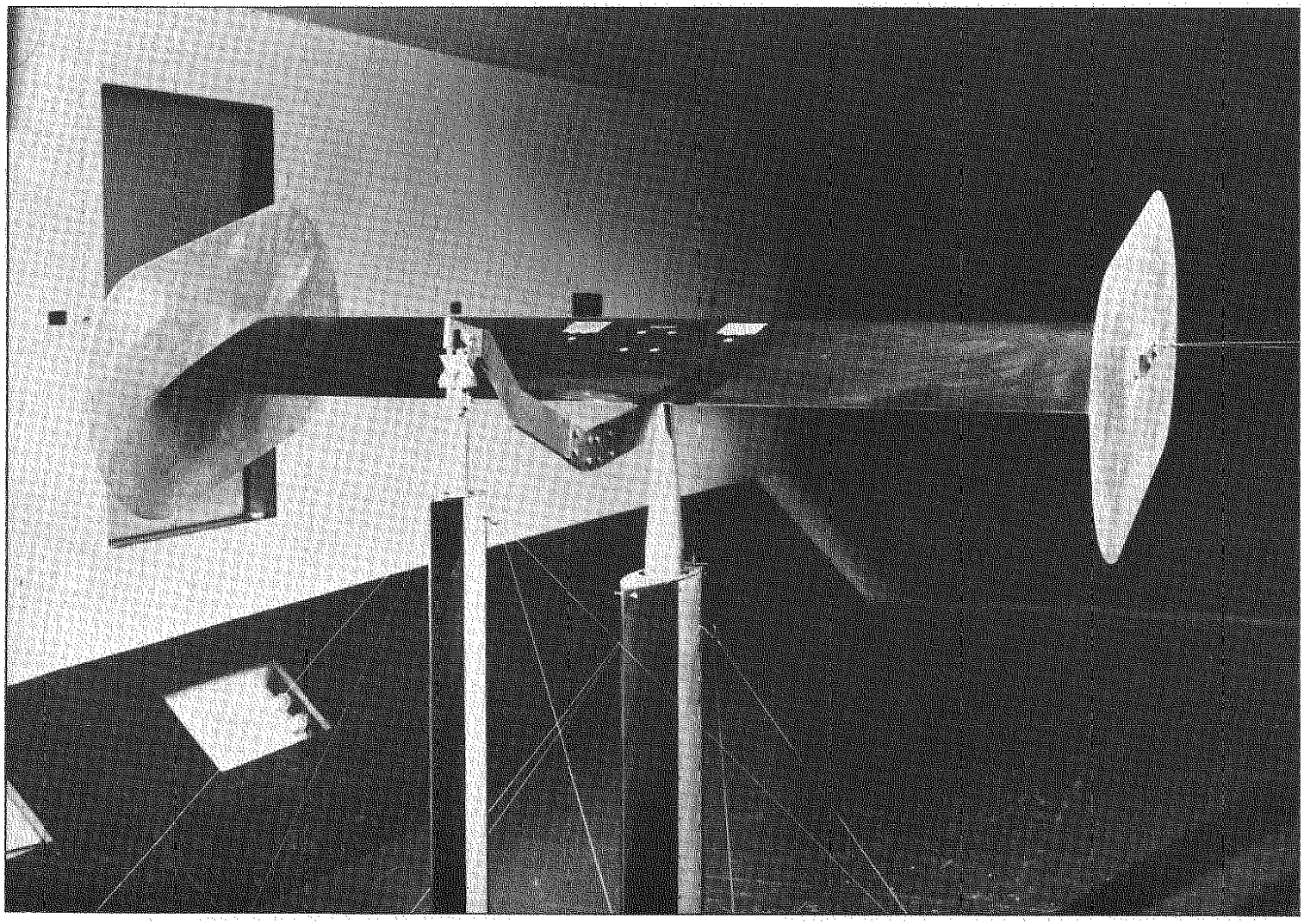

Fig.2 Preliminary test arrangement (model with end-plates)

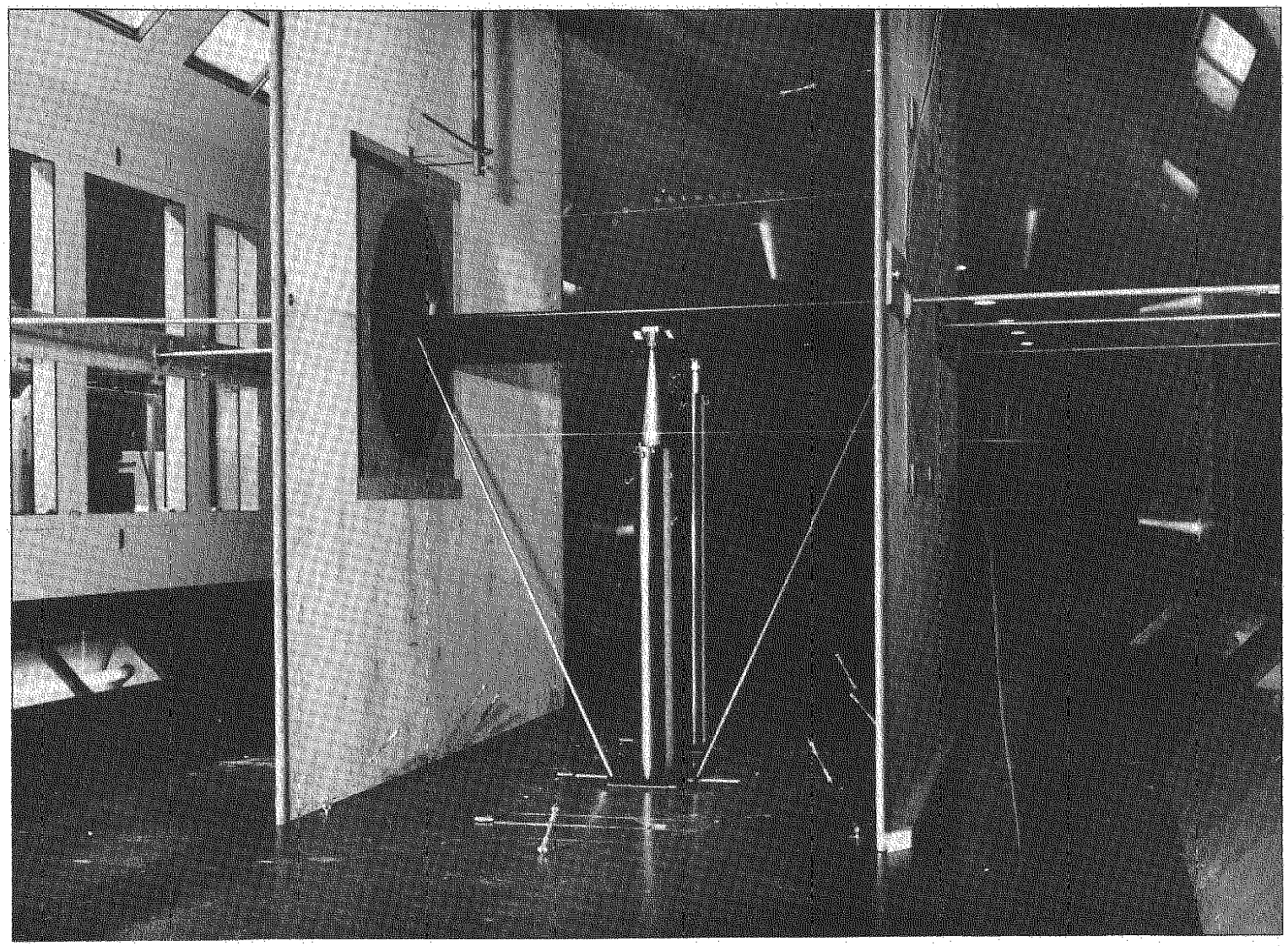

Fig.3 Final arrangement in the 13ft.x9ft. tunnel (wing between false walls)

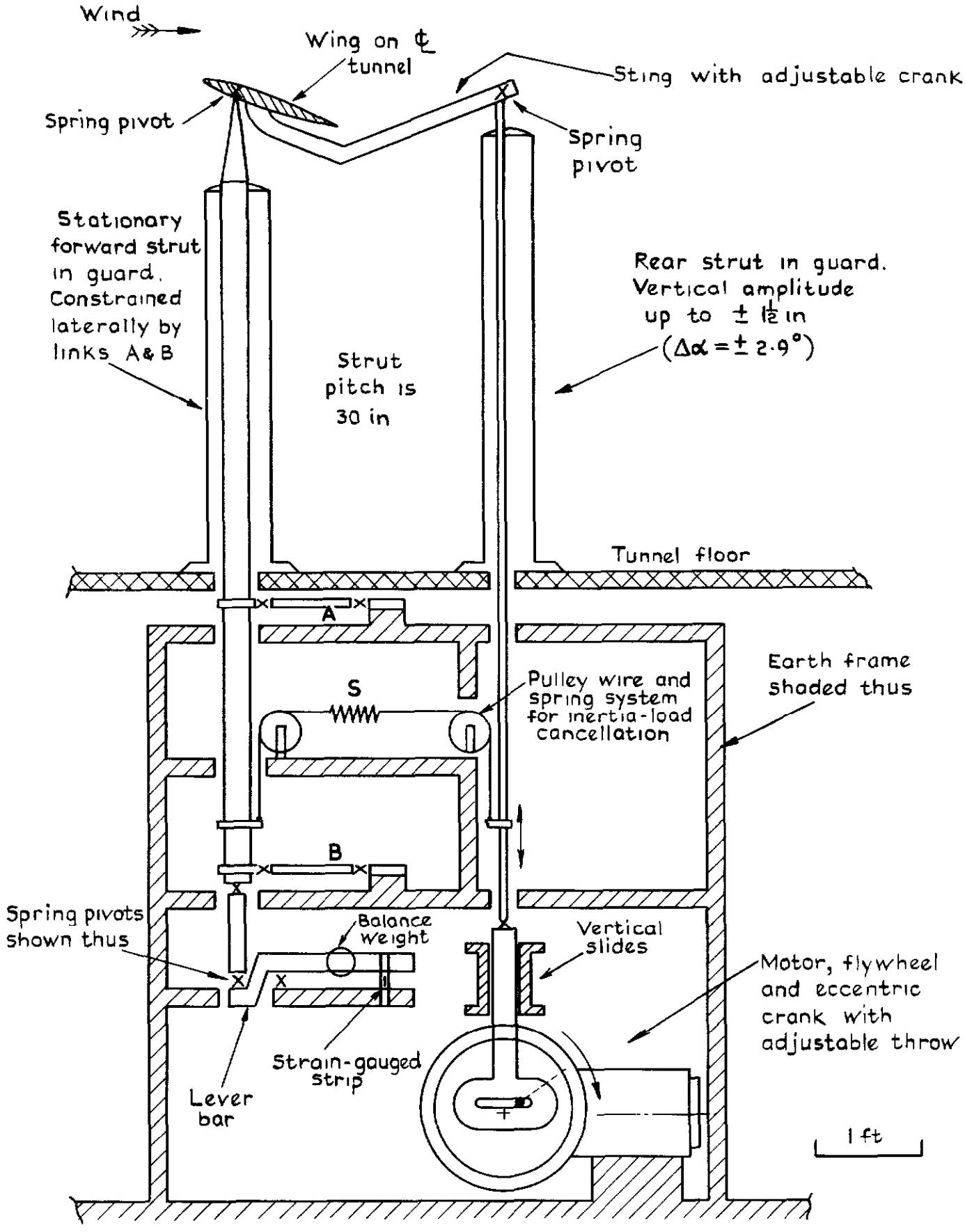

Fig 4 Semi-diagrammatic sketch of balance and oscillating rig

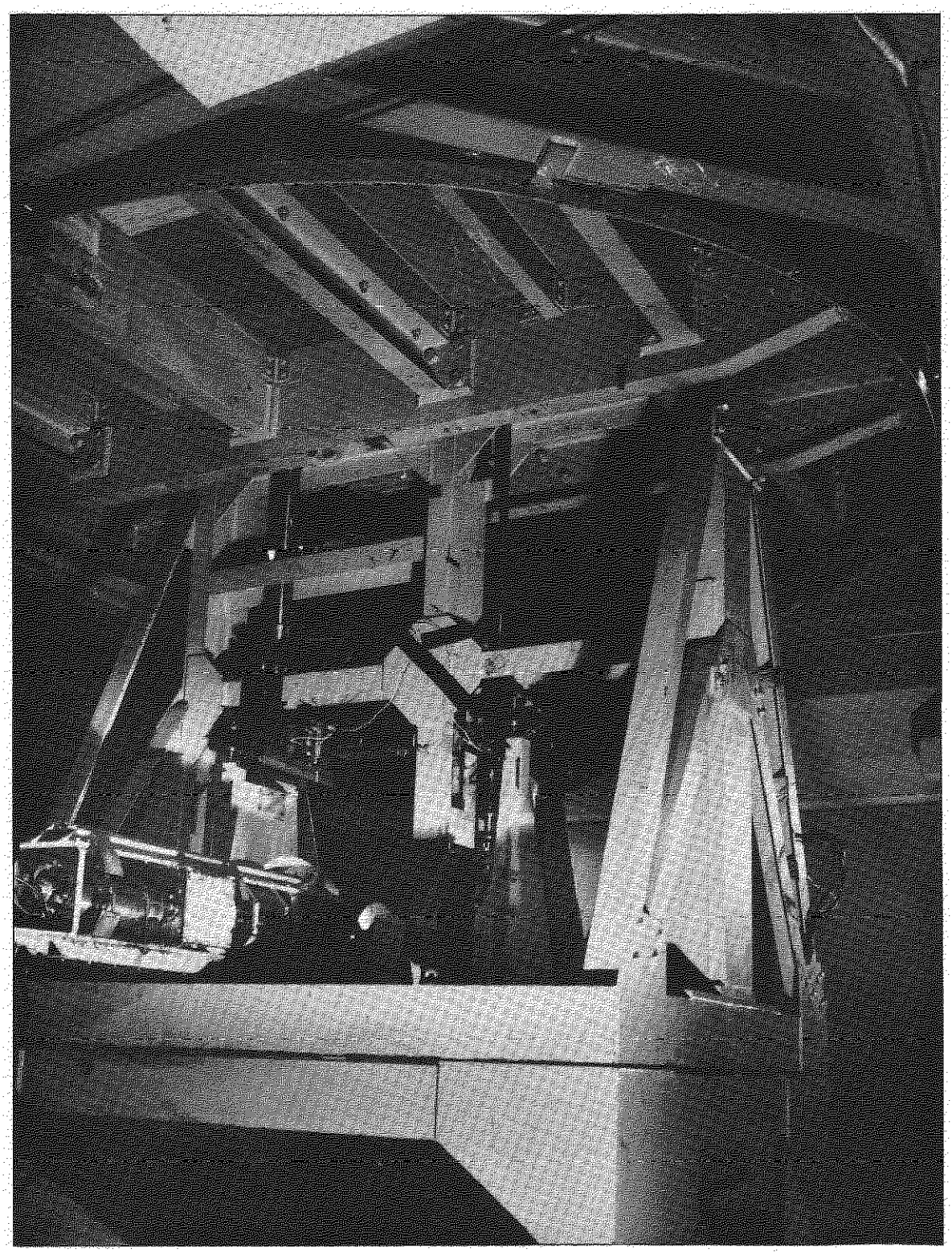

Fig.5 Balance and oscillating rig

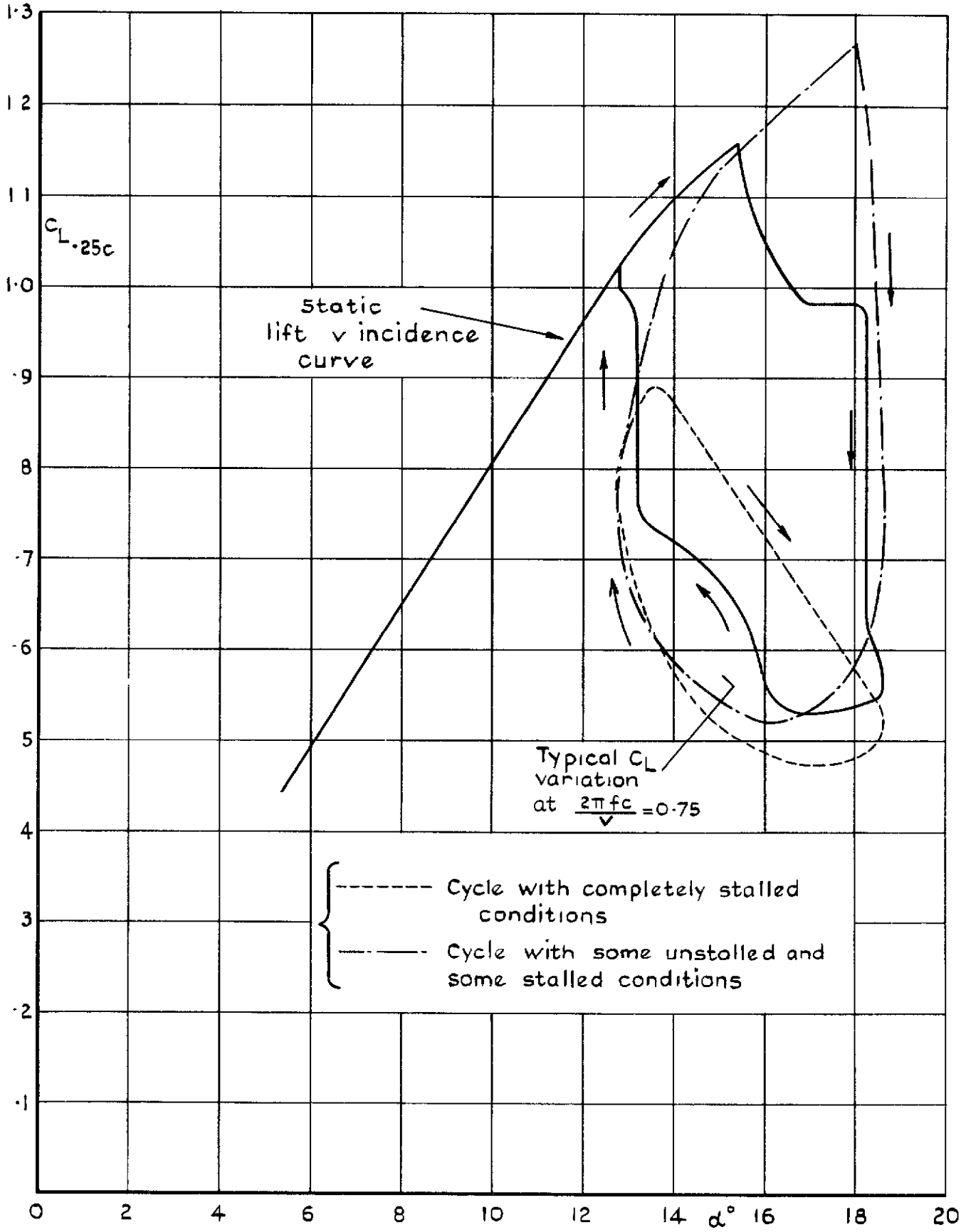

Transition free · V=100ft/sec : $\frac{2\pi fc}{V} = 0.75 : 12.8° < \alpha < 18.6°$

Fig 6 Typical C_L v α variation for wing with endplates [Preliminary test series]

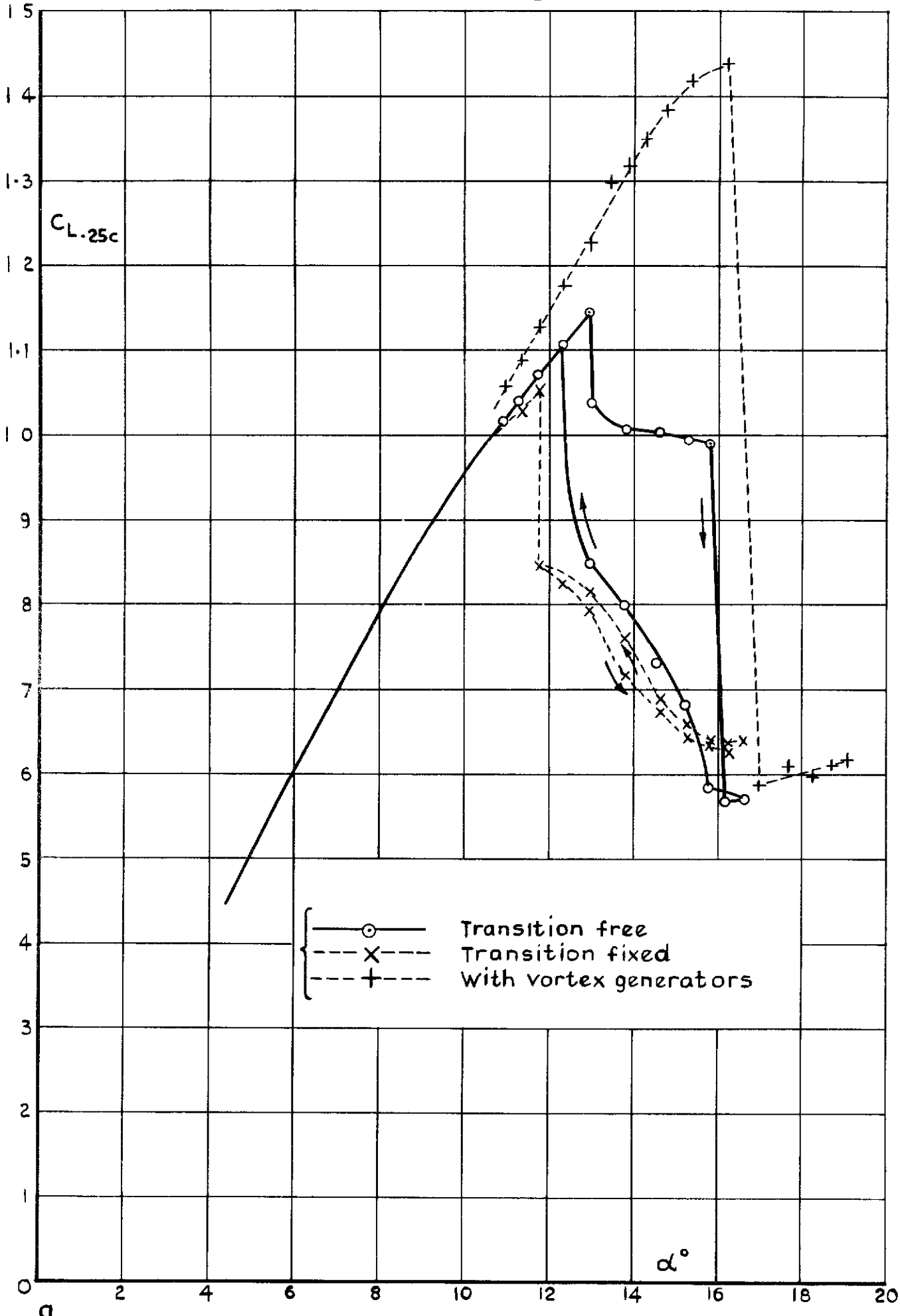

a

Fig. 7a Static tests : V = 100 ft/sec C_L v α

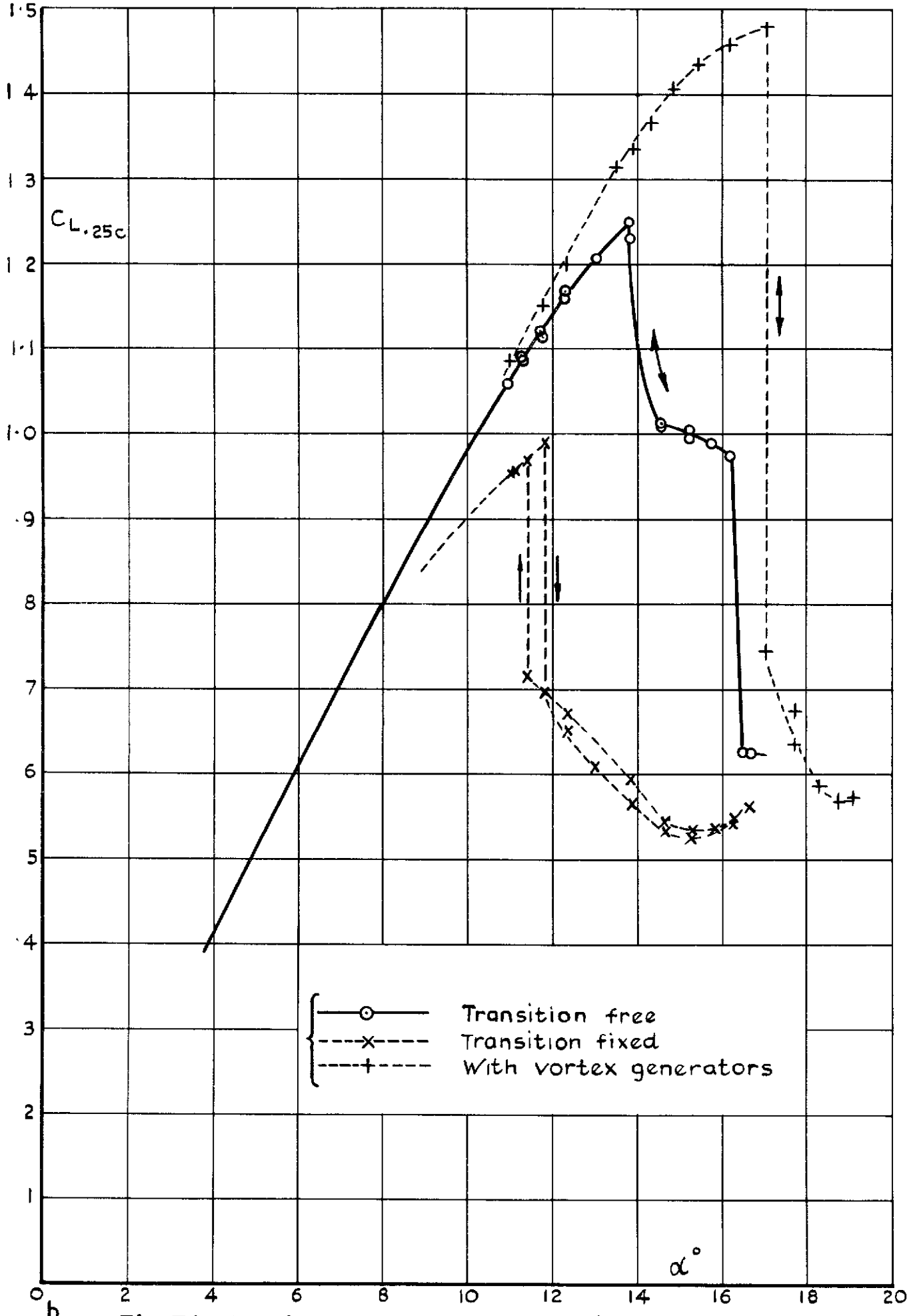

b

Fig 7b Static tests : V=200ft/sec C_L v α

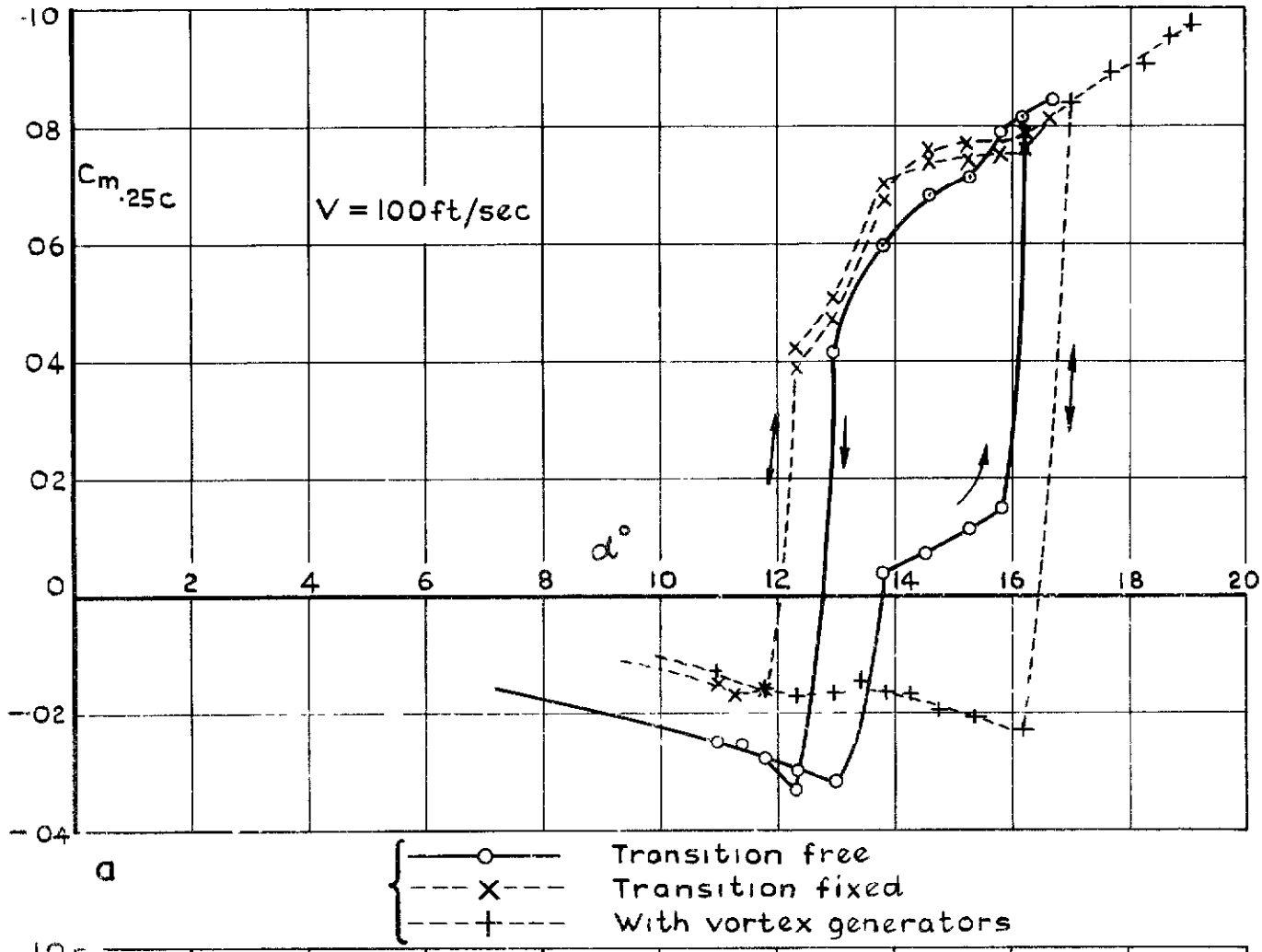

Transition free
Transition fixed
With vortex generators

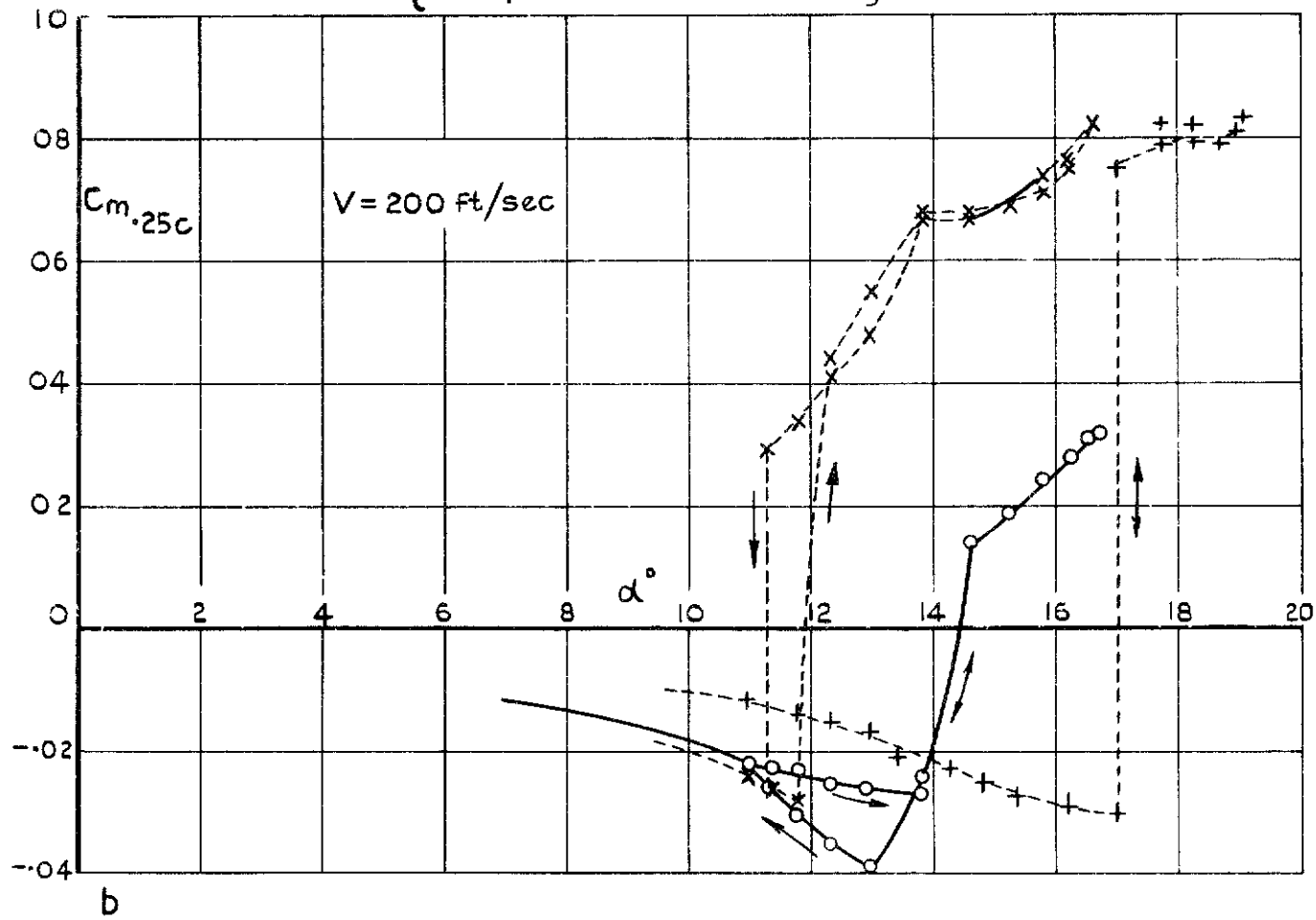

Fig. 8 a & b Static tests: C_m v C_L

$\alpha = 12.3^{\circ}$

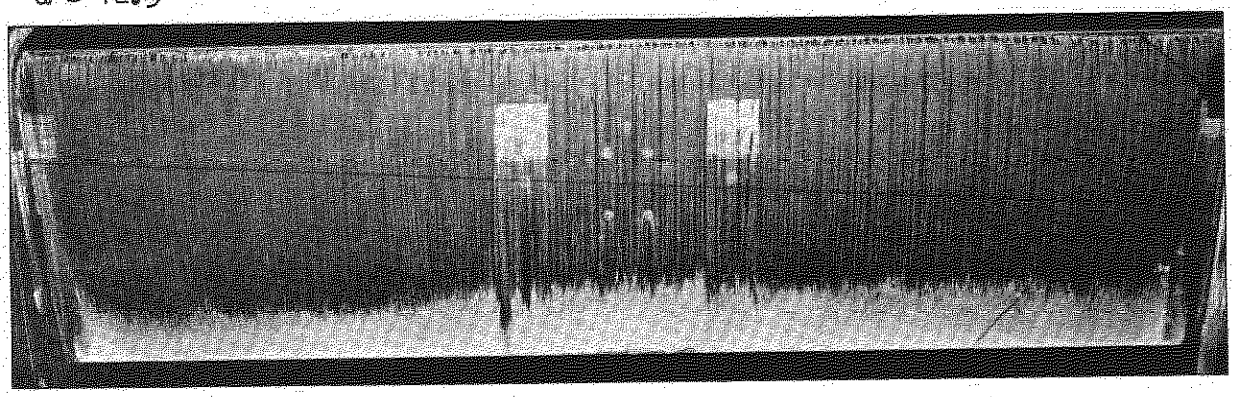

$\alpha = 14.6^{\circ}$

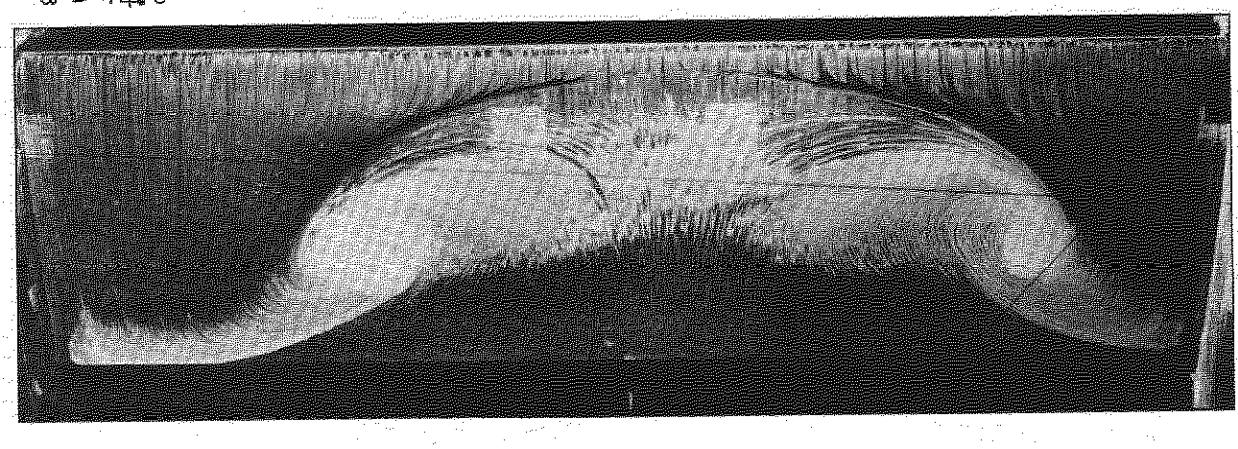

$\alpha = 16.6^{\circ}$

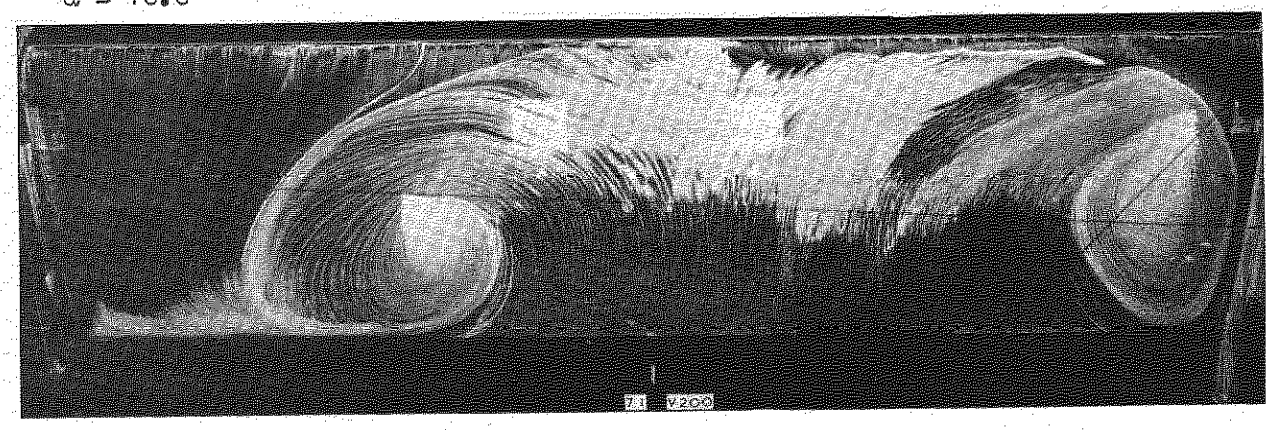

Transition free: V=200F.P.S.

Fig.9a Static upper-surface oil flow photographs

$\alpha = 10.95^{\circ}$

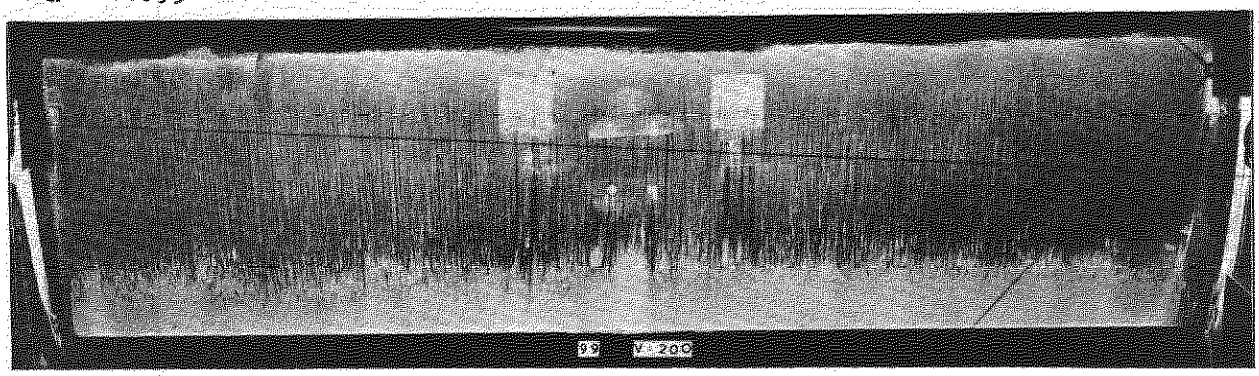

$\alpha = 12.3^{\circ}$

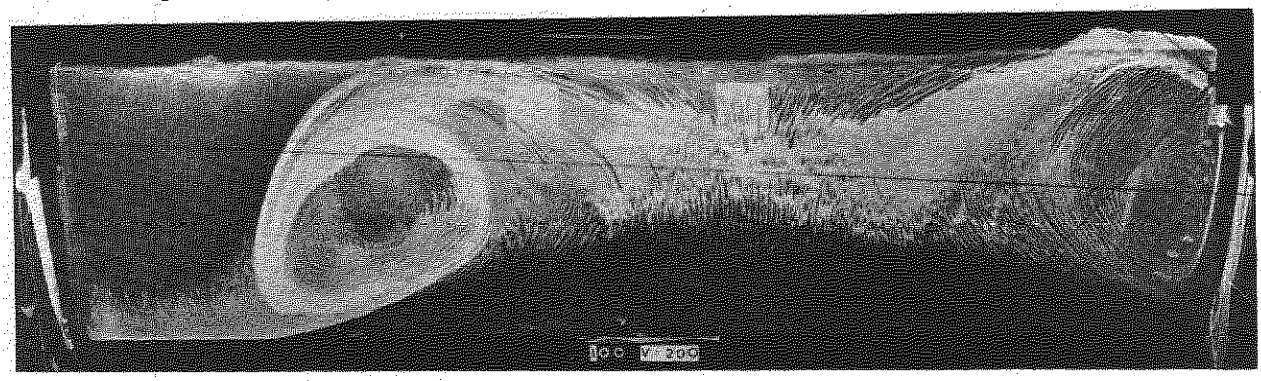

$\alpha = 16.6^{\circ}$

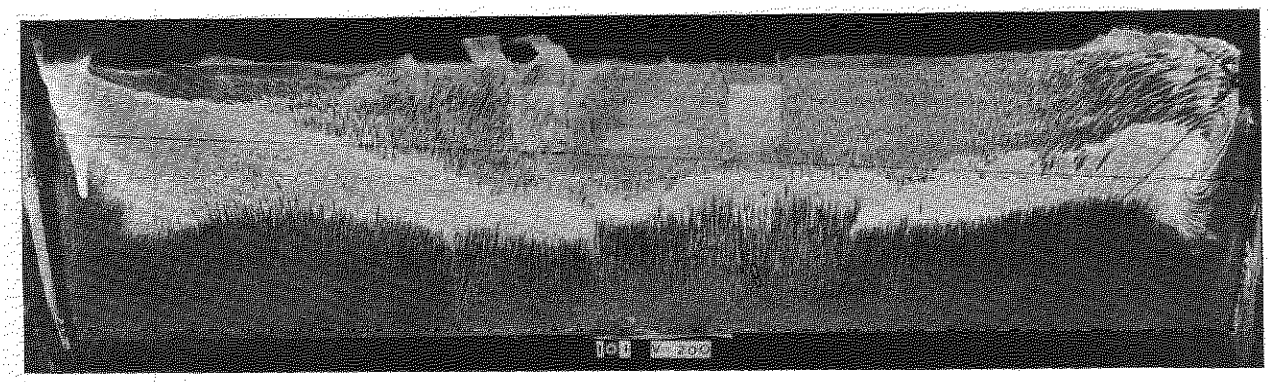

Transition fixed: V=200F.P.S.

Fig.9b Static upper-surface oil flow photographs

$\alpha = 14.2^{\circ}$

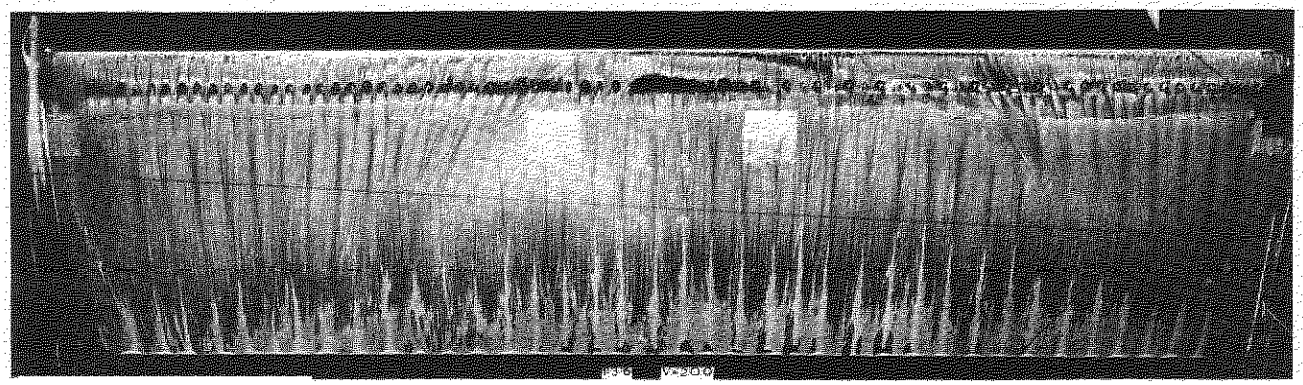

$\alpha = 16.2^{\circ}$

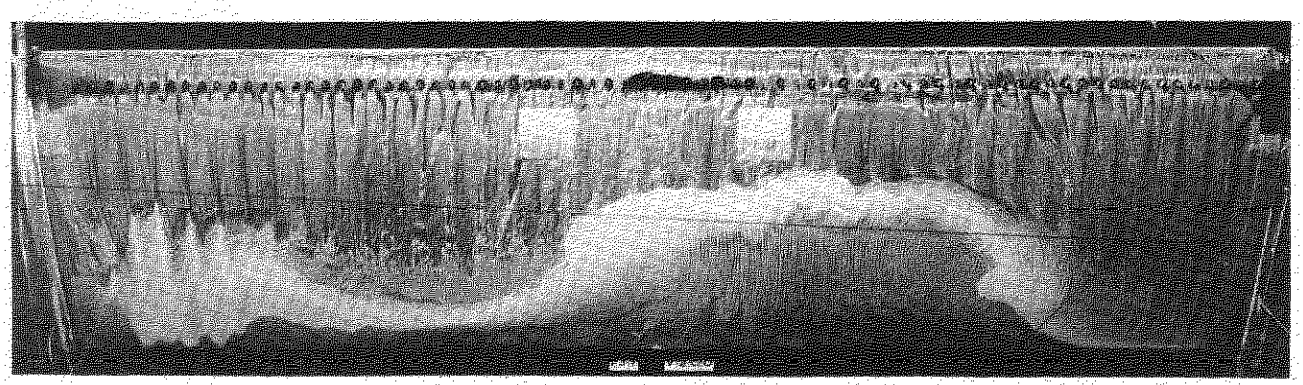

$\alpha = 19.1^{\circ}$

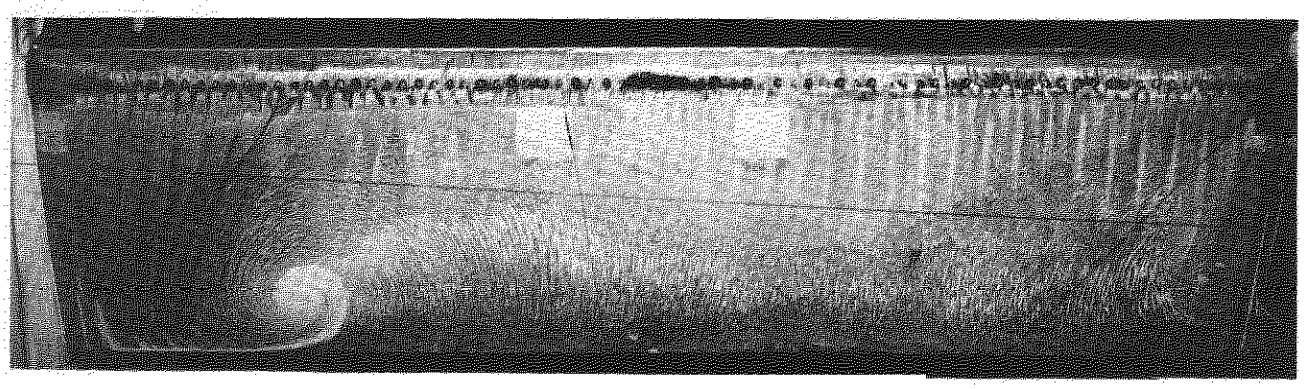

With vortex generators: V=200F.P.S.

Fig.9c Static upper-surface oil flow photographs

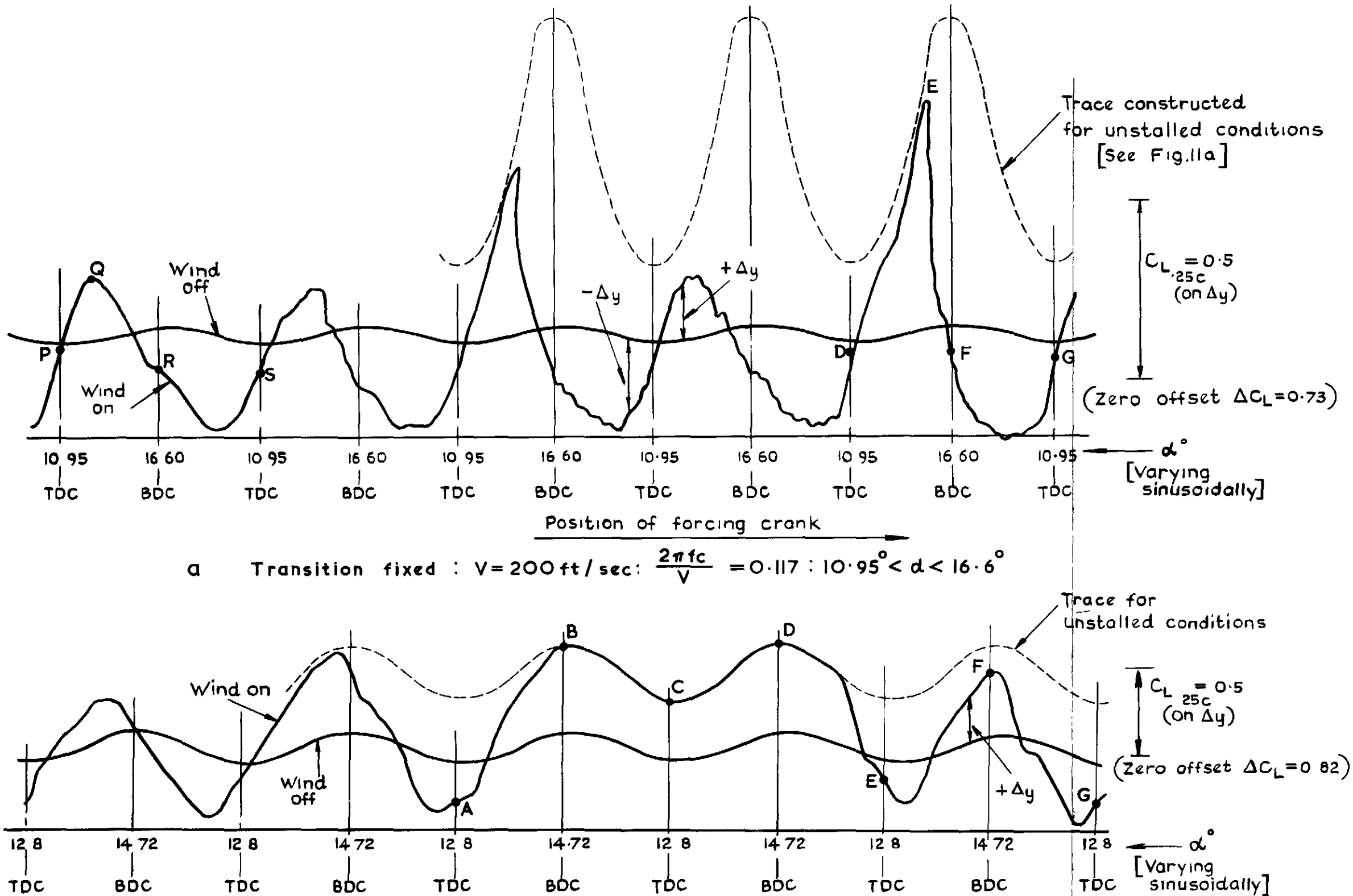

Fig 10 a&b Typical recorder traces : strain-gauge signal from forward-strut balance

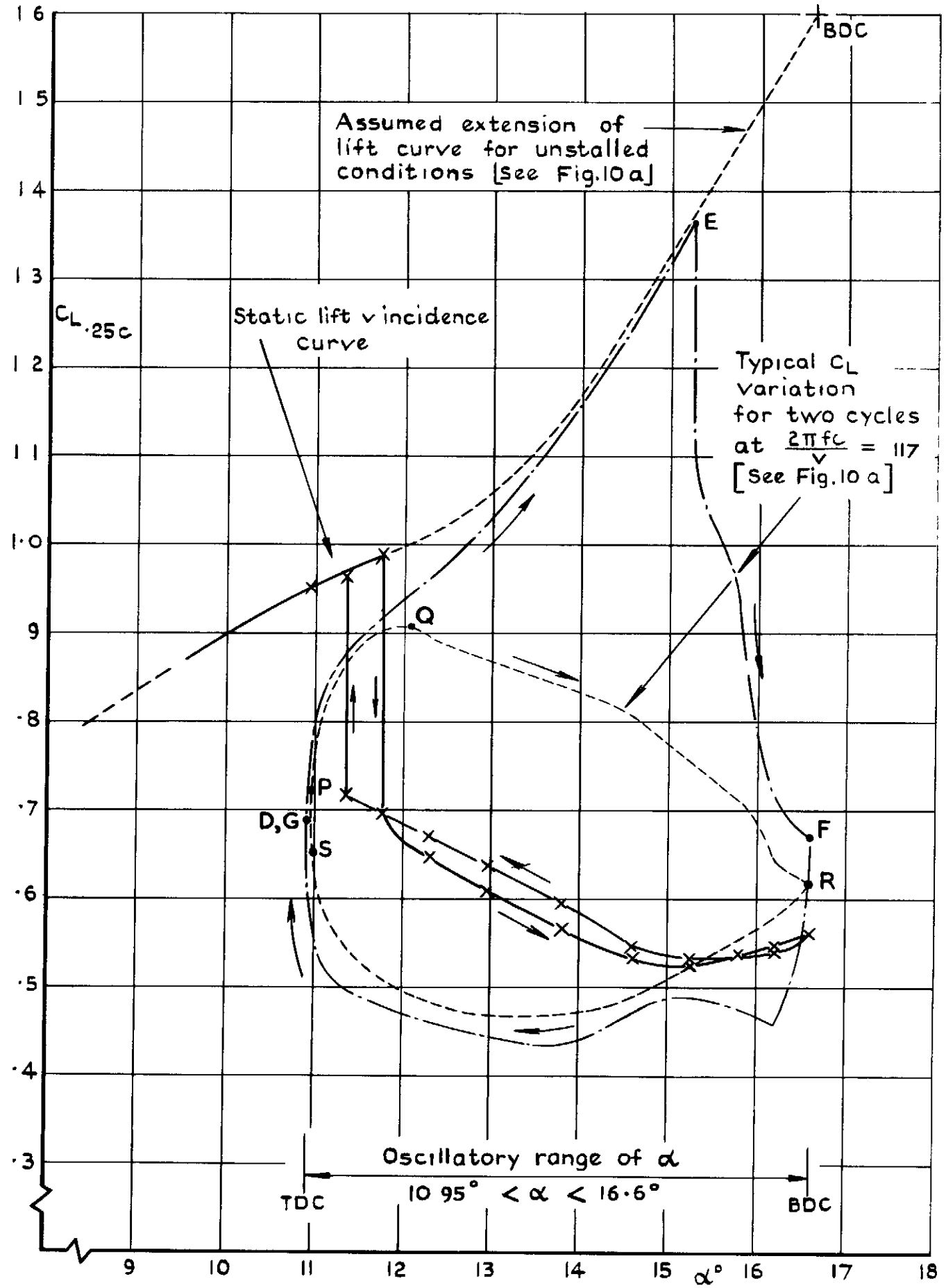

a Transition fixed : V=200 ft/sec : $\frac{2\pi fc}{V} = 0{\cdot}117$: $10{\cdot}95 < \alpha < 16{\cdot}6$

Fig.11a Typical C_L v α plots under oscillatory conditions

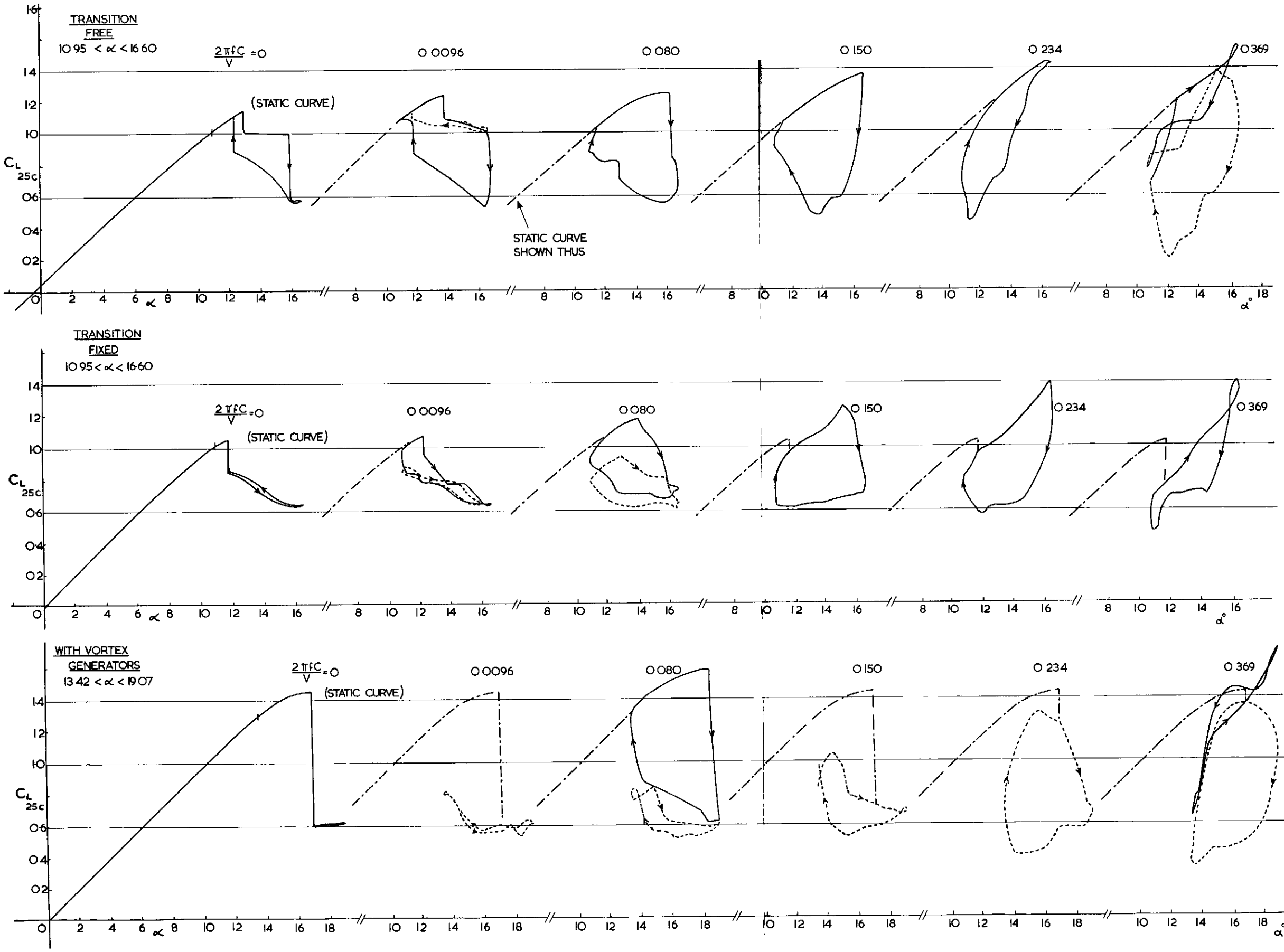

FIG. 12 (a): VARIATION OF C_L WITH INCIDENCE UNDER OSCILLATORY CONDITIONS

V = 100 ft/sec.

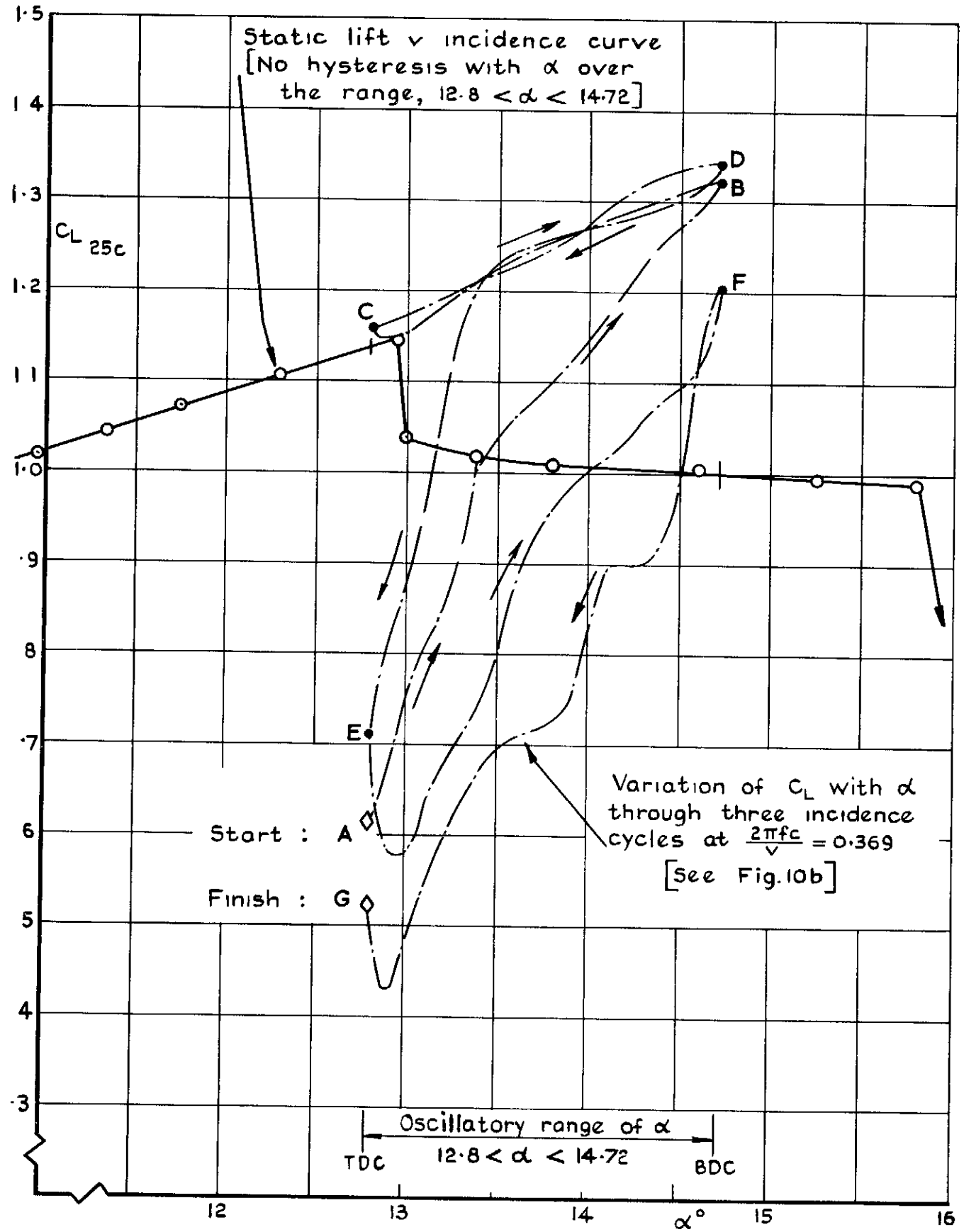

b Transition free : V=100ft/sec : $\frac{2\pi fc}{V} = 0.369$: $12.8^\circ < \alpha < 14\ 72^\circ$

Fig.11b Typical C_L v α plots under oscillatory conditions

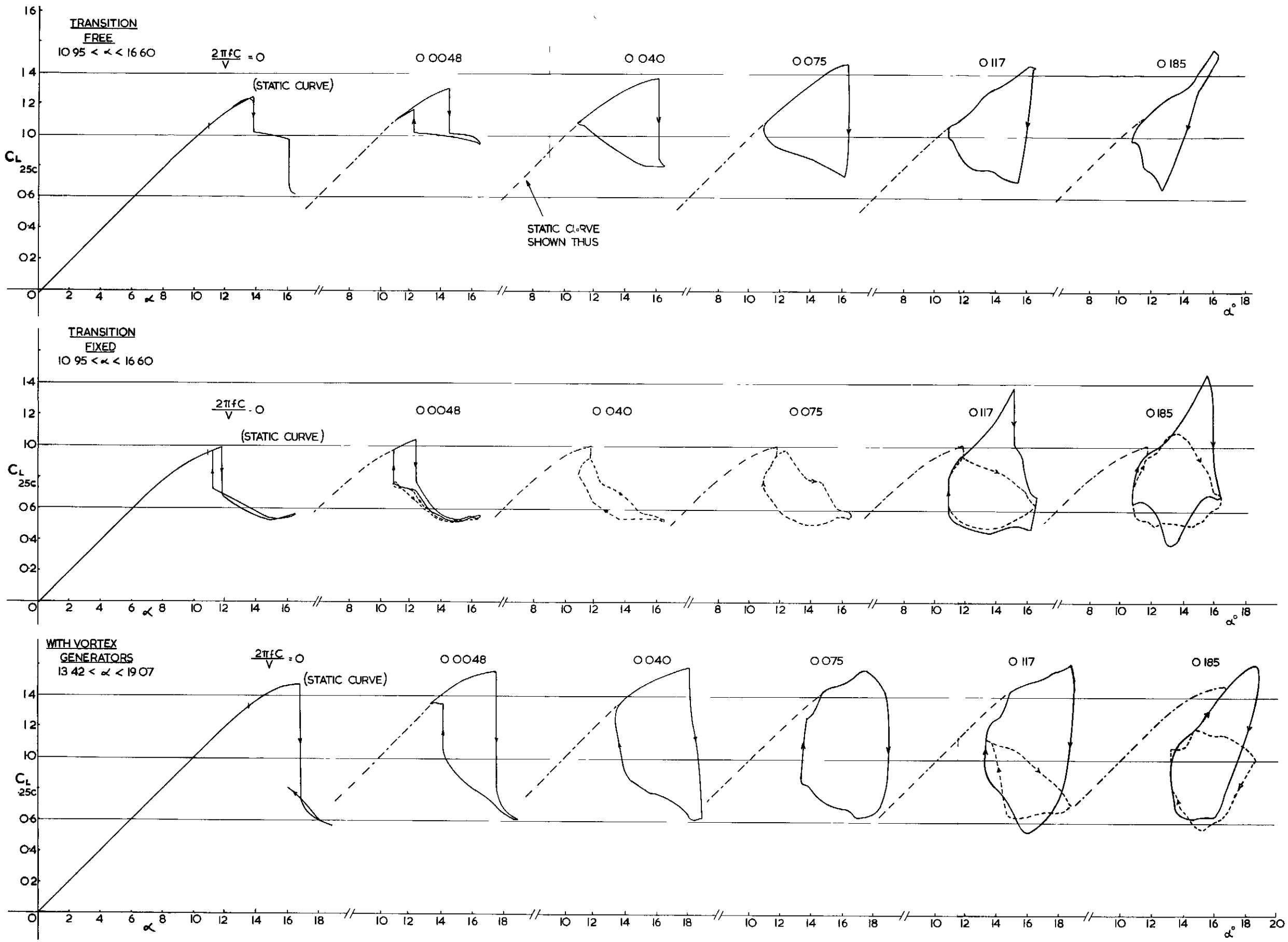

FIG. 12 (b): VARIATION OF C_L WITH INCIDENCE UNDER OSCILLATORY CONDITIONS

V = 200 ft/sec.

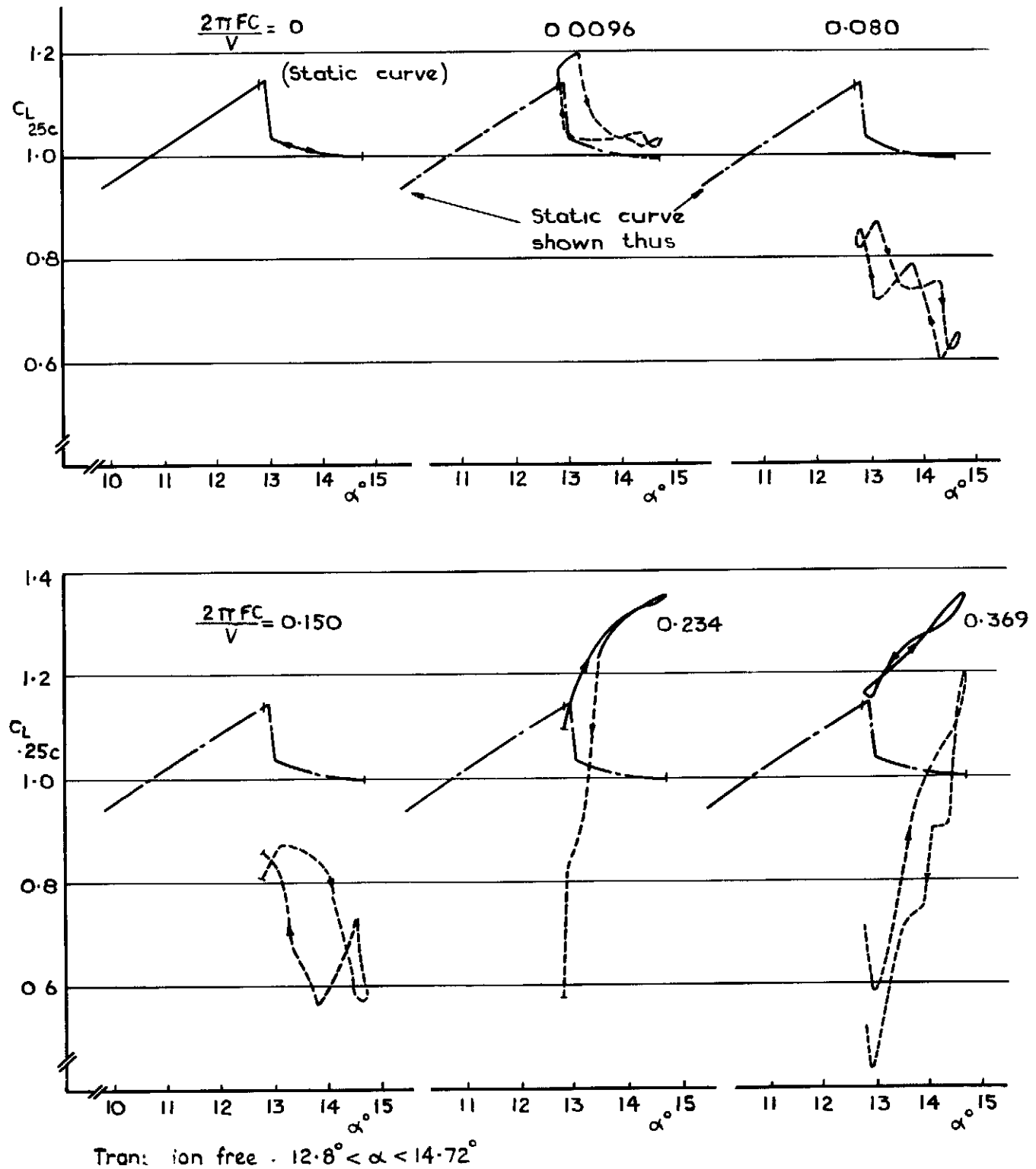

Fig. 12 c Variation of C_L with incidence under oscillatory conditions

V = 100 ft/sec

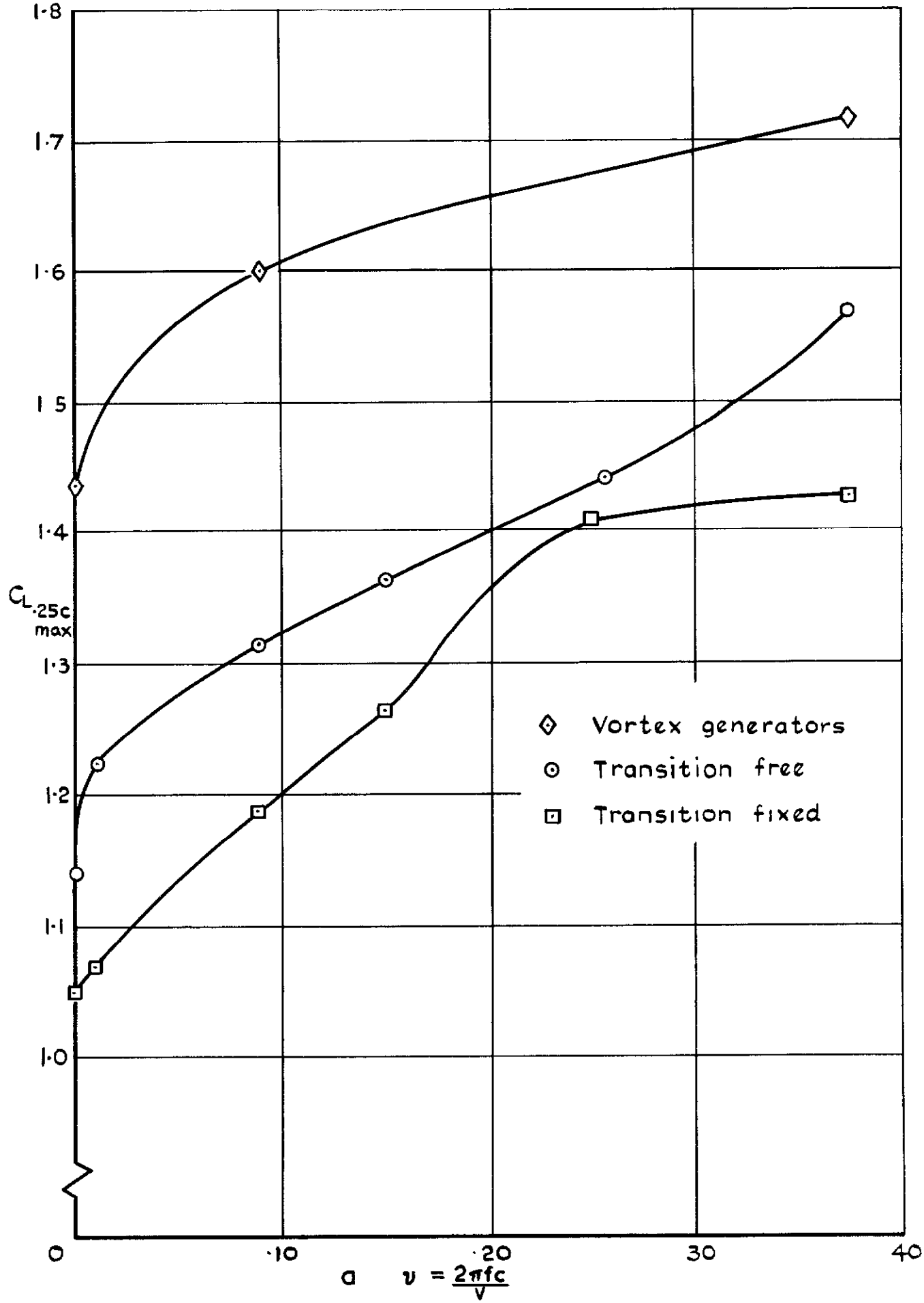

Fig. 13a $C_{L\,max}$ v $\frac{2\pi fc}{V}$ · V = 100 ft/sec

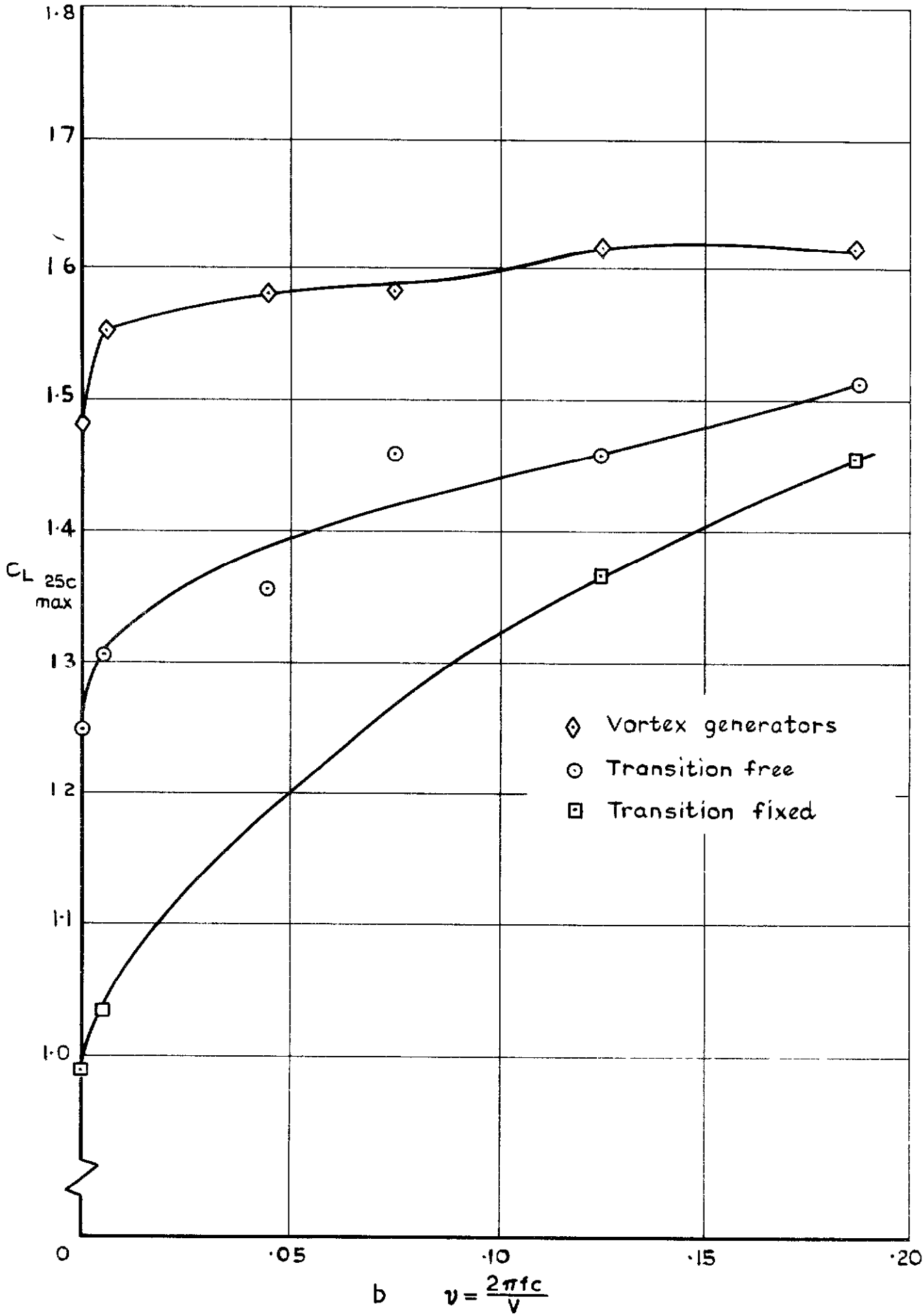

Fig. 13 b $C_{L max}$ v $\frac{2\pi fc}{V}$: V = 200 ft/sec

Printed in England for Her Majesty's Stationery Office by the Royal Aircraft Establishment, Farnborough Dd 501371 K 4

DETACHABLE ABSTRACT CARD

A.R.C C.P. No.1145
May 1968

Moss, G F
Murdin, P M.

533.692
533 6 013 13
533 6.071
533.6 011 32/34
533 6 013 152
629 13.038 1

TWODIMENSIONAL LOW-SPEED TUNNEL TESTS ON THE N.A C.A. 0012 SECTION INCLUDING MEASUREMENTS MADE DURING PITCHING OSCILLATIONS AT THE STALL

Lift measurements were made on a 10% thick N A.C.A 0012 section under static conditions and during pitching oscillations in an attempt to provide sectional data for use in calculations on helicopter rotors Strong threedimensional effects were found at the stall, however, which seemed to be inherent in the aerodynamics of the stall itself Also, the cyclic variation of lift during the pitching oscillations was found to be intermittent between two distinct types during both of which considerable hysteresis was observed and during one of which very large increases in maximum lift were encountered

A.R C C.P No.1145
May 1968

Moss, G F.
Murdin, P M

533 692
533 6 013 13
533 6 071
533 6 011 32/34 :
533.6.013 152 ·
629.13 038 1

TWODIMENSIONAL LOW-SPEED TUNNEL TESTS ON THE N.A.C.A 0012 SECTION INCLUDING MEASUREMENTS MADE DURING PITCHING OSCILLATIONS AT THE STALL

Lift measurements were made on a 10% thick N A C A 0012 section under static conditions and during pitching oscillations in an attempt to provide sectional data for use in calculations on helicopter rotors Strong threedimensional effects were found at the stall, however, which seemed to be inherent in the aerodynamics of the stall itself Also, the cyclic variation of lift during the pitching oscillations was found to be intermittent between two distinct types during both of which considerable hysteresis was observed and during one of which very large increases in maximum lift were encountered

Published by
HER MAJESTY'S STATIONERY OFFICE

To be purchased from
49 High Holborn, London WC1 V 6HB
13a Castle Street, Edinburgh EH2 3AR
109 St Mary Street, Cardiff CF1 1JW
Brazennose Street, Manchester M60 8AS
50 Fairfax Street, Bristol BS1 3DE
258 Broad Street, Birmingham B1 2HE
80 Chichester Street, Belfast BT1 4JY
or through booksellers

C.P. No. 1145

SBN 11 470393 0